ISLAMIC UNIVERSITY OF TECHNOLOGY

ORGANISATION OF ISLAMIC COOPERATION

NUMERICAL INVESTIGATION OF LOCAL SCOUR AROUND DIFFERENT SHAPED BRIDGE PIERS USING FLOW-3D SOFTWARE

B.Sc. Engineering (Mechanical) Thesis

Authored by

RAKIB HASAN

Student ID: 151434

ROWFI KHAN

Student ID: 151419

SUPERVISED BY

PROF. DR. MD. HAMIDUR RAHMAN

Department of Mechanical and Production Engineering (MPE)

Islamic University of Technology (IUT)

DEPARTMENT OF MECHANICAL AND PRODUCTION ENGINEERING (MPE)

Islamic University of Technology (IUT)

NOVEMBER 2019

CERTIFICATE OF RESEARCH

This thesis titled **"NUMERICAL INVESTIGATION OF LOCAL SCOUR AROUND DIFFERENT SHAPED BRIDGE PIERS USING FLOW-3D SOFTWARE"** submitted by **RAKIB HASAN (151434)** and **ROWFI KHAN (151419)** has been accepted as satisfactory in partial fulfillment of the requirement for the Degree of Bachelor of Science in Mechanical Engineering on November 2019.

Supervisor

_____

PROF. DR. MD. HAMIDUR RAHMAN
Department of Mechanical and Production Engineering (MPE)
Islamic University of Technology (IUT)

Head of the Department

_____

PROF. DR. MD. ZAHID HOSSAIN
Department of Mechanical and Production Engineering (MPE)
Islamic University of Technology (IUT)

Candidate's Declaration

It is hereby declared that, their thesis or any part of it has not been submitted elsewhere for the award of any degree or diploma.

Signature of the Candidate's

RAKIB HASAN

Student ID: 151434

ROWFI KHAN

Student ID:151419

Department of Mechanical and Production Engineering(MPE)
Islamic University of Technology (IUT)
Board Bazar, Gazipur-1704
Dhaka, Bangladesh

Signature of the Supervisor

PROF. DR. MD. HAMIDUR RAHMAN

Department of Mechanical and Production Engineering(MPE)

Islamic University of Technology(IUT)

Acknowledgments

We would like to express our sincere thanks to our respected supervisor Prof. Dr. Md. Hamidur Rahman sir for his continuous support and guidance throughout this research period and our undergraduate study. His motivation and advice helped us a lot in every step of this research work and writing of this thesis book. His constructive comments helped us a lot to understand and complete this research work.

We are also grateful to our beloved parents for their continuous encouragement and support.

Table of contents

List of Figures

List of Tables

Nomenclature

τ_o= bed shear stress(Pa)

τ_c= critical shear stress(Pa)

R_{*c}= Shear Reynolds number

τ_{*c}= Non-dimensional shear stress

u_{*c}= shear velocity at the critical condition (m/s)

Υ = unit weight of water(N/m^3)

Υ_s= unit weight of sediment particle(N/m^3)

ν = kinematic viscosity of water (Ns/m^2)

d_{50}= mean diameter of sand particle(mm)

Θ_n= critical shield parameter

g = acceleration of gravity(m^2/s)

ρ= density of water(kg/m^3)

ρ_s= density of sand(kg/m^3)

$d_{*,n}$= dimensionless grain size

Φ_n= dimensionless bed load transport parameter

B_n = the bed load coefficient

$C_{s,n}$= suspended sediment mass concentration

t = time(sec)

Abstract

Scour is one of the most protruding factors in bridge failures across the whole world. In this paper, we have studied about the scouring around bridge piers of different hydrodynamic geometries such as circular, square, diamond, hexagonal and airfoil. And it has been done with the help of using FLOW-3D software. In this analysis we have tried to investigate whether Flow-3d can accurately predict the scouring geometry, the depth and deposition of sand around bridge piers or not. In this study mainly the scouring in case of non-cohesive bed sediment was simulated using the software where both the qualitative and quantitative analysis have been presented. And the software uses Reynold's Average Navier Stokes (RANS) equation closed with k-€ model with second order accurate turbulence method. The computational model has established stable and converged solution for different shapes of hydrodynamic structures with a constant time interval and fixed bed load coefficient and the result is satisfactory enough to build up a consensus about the scouring pattern and depth as well as the deposition in some portion around the piers. The study gives a conclusion which suggest that among the different five shapes (circular, square, diamond, hexagonal, airfoil), for circular shape the scour depth is satisfactory than other diamond and hexagonal shape but in case of airfoil scouring is so high that it didn't catch our thought anyway. Besides these, it also shows that scouring is higher in the upstream of the piers than the downstream. Another major finding of our work is that there are some limitations in the Flow-3d software to predict the scouring depth.

Keywords: *local scour, horseshoe vortex system (THSV), scour depth, bed topography, CFD, non-cohesive sand, deposition height, critical shields number.*

Chapter 1 Introduction

Scouring is a very general and common phenomena which occurs in the rivers or other steams and causing the breakdown and failures of many bridges of the world. The study on scouring is developing day by day and it can't be fully removed rather the measure of erosion and bridge failure can be reduced with the help of adapting some measures. Local scour occurs due to the heavy pressure flow on the upstream of the riverside which creates horse shoe vortex around the sets of piers and by the influence of the pillars and high shear stress the underneath sands are moving from the region and creates an area where the supportive non cohesive soil is not present causing the bridge to fail. And extensive work around the world is going on to reduce the failures of bridges. Flood or the increased water flow which at the same time increases the pressure on the structure causes the downward movement of the sand layer around bridge levels and some areas around the pillars of the bridges. Formation of scour pit for flooded condition is playing a vital role in the erosion process.

Figure 1: Scouring effect around a bridge pier[16]

Scouring processes are not easy to predict because it is a very multifarious in nature and which also depends on various parameters that are not easy or sophisticated to control. The behavior of these parameters are also not stable, so a gradual development and analysis are required to get a good control on these variables. Countless flume experiments have been done on the laboratory which generates a method to develop and reduce the failures which causes a lot of money halt. Briaud et al. [1], for instance, explore that as of 1999 more than 1000 of about 600,000 bridges in the United States failed with 60% of these failures being due to scour. Scouring also effects the wind firm and other heavy structural failures of large installation cost.

(a)

(b)

Figure 2: Bridge failure due to scouring effect both (a) & (b)[17]

In the field of scouring many researchers have studied the various aspects of local scour like temporal and equilibrium scour (Melville and Chiew 1999[31], Kothiary et al 1992a[32], Johnson and Bilal 1992[33], Laursen 1963[34]), clear water and live bed scour (Vittal et al 1994[35], Jain 1981[36], Kothiary et al 1992b[37], Laursen 1962[38]), scour in uniform and non-uniform bed materials (Melville and Chiew 1999[31], Molinas and Abdeldayem 1998[39], Raudkivi and Ettema 1977[40]), scale effects in pier scour (Kabir et al 2000[41], Laursen 1963[34], Laursen 1962[38]) and so on. Again many empirical equations (Kandasamy and Melville 1998[42], Melville and Sutherland 1988[43], Poona (Chang 1988[44], Garde and Raju 1985[45]) and mathematical models (Ram 1999[30], Johnson and Bilal 1996[46],Dey et al 1995[47]) are available for predicting pier scour depth, which are usually intended to estimate the ultimate scour depth. More recently attempts were made to reduce scour with the piers of different shape, geometry and orientation (Sheppard and Jones 1998[48], Kumar et al 1999[49],Parola 1996[50], Lim and Chiew1999[51])

Baker [2] was the one who first came up with the turbulent horseshoe vortex system (THSV) which develops in the upstream side of a circular pier with a flat, rigid bed for Reynolds numbers up to 90,000 (based on the pier diameter D and the approach flow velocity) and was able to identify primary and secondary vortical structures wrapping around the pier. And with the help of this study, several others study based on the THSV system around circular piers with fixed bed condition had been done by Devenport and Simpson [3], Agui and Andreopoulos [4], Doligalski et al. [5] and Seal and Smith [6]. Martinuzzi and Tropea [7] and Hussein and Martinuzzi [8] have studied about the flow pattern and scouring around square and rectangular piers for fixed bed rigid state. Recently a very noteworthy study by Unger and Hager [9] who carried out particle image velocimetry (PIV) experiments of bridge pier flows over a wide range of Reynolds numbers and their study came to a conclusion that strong flow velocity and the turbulent horse shoe vortex system (TSHV) are the main reasons for scouring around the bridge piers. Up to now we have been discussed about the various experimental studies and researches on the field of scouring. In addition of these many computational studies with fixed bed and mobile bed as well as many different shapes of the piers and nature of the sand have been in the interest of study. The

computational studies are based on Reynold's Average Navier Stokes equation which solves the computational domain with maximum accuracy focusing on flow patterns around piers on a flat rigid bed have been reported by Mendoza-Cabrales [10], Richardson and Panchang [11], Tseng et al. [12], Nurtjahyo [13], Ge and Sotiropoulos [14], and Salaheldin et al. [15].

Scouring around the bridges is one of the most prominent causes for bridge failures. According to a study by Shirhole and Holt (1991)[18], in the past 30 years more than 1,000 bridges collapsed in the United States and about 60% failures are related to the scouring around the bridge piers. This problem has been severe after a study done by the Transportation Research Board in 199, there were 488,750 bridges over streams and rivers in the U.S. and the annual cost for scour related bridge failures was estimated at $30 million (Lagasse et al. 1997)[19]. According to the study of Alabi (2006)[20] which stated that the average cost for flood damage repair of the United States highways was $50 million per year.

Additionally, it was estimated that at least $20 million have been invested on scour research in the United States in the last two decades (Briaud et. al, 2012)[21]. Alabi (2006)[20] also cited that the associated repair costs of the bridge collapse in 1993 (due to scour) in the upstream Mississippi and downstream Missouri river basins were more than $8,000,000. The economic losses for this scouring are gigantic and which arrest a lot of money of the government as well as the risk became massive. And for that reason Scientists and Researchers are working for many years to minimize the risk potential and the scouring effect by minimizing the strength of the horse shoe vortex which is one of the most mentionable cause for the scouring around the bridges pillars. In this paper we will do a comparative study between the different structures of the bridge pillars and their effect on scouring.

Thus the main objectives of our study is to investigate the scouring effect for different shapes of the pillar structures like circular, square, diamond, hexagonal and airfoil and to do a comparative analysis between these structures to find a conclusion of which one is better in implementing as pillar structure. We will also investigate the causes of the scouring and the variation in their equilibrium scour depth for different hydrodynamic structures. This numerical analysis will make a way to the reduction process of scour depth. For the numerical analysis, grid sensitivity study has been carried out to investigate the numerical errors due to the discretization of the governing equations.

We will also discuss on the grid refinement study and their effect on the equilibrium scour depth as well as equilibrium bed elevation. For the numerical simulation, time effects are so important in comparing the scour depth and elevation for all of the structures and for that simulation has been carried out until the scour depth reaches an equilibrium condition. In summary it mainly discussed the scour evolution under the flooded bridge piers for different structures and this study has been done based on computational fluid dynamics using FLOW -3D which can predict the scouring more precisely.

Chapter 2 Literature Review

Scouring causes the movement of the sediment bed from the upstream of the flow direction and the movement weakens the pillar structure and making the structure risky. It has been studied for the past few decades and being continued. This chapter will specially discuss on the basic theories related to the transportation of the sediment and the different types of scouring and its related things.

2.1 Basic theory related to scouring:

The alluvium or sediment refers to the loose and no cohesive element which usually move due to the action of water with varying velocity and resulting deposition or transportation of it. Sediment doesn't move only because of the action or flow of water, it unquestionably needs a minimum or threshold force for the movement of the sediment whether it is deposition or transportation. And the Initiation of the motion of the sediment depends upon the bed shear stress which can be defined as

$$\tau_o = \Upsilon R S_O \text{ [22]} \ldots\ldots\ldots\ldots\ldots\ldots\ldots\ldots (1)$$

From the different experimental analysis, it has been seen that for the low range values of the bed shear stress there has no movement of the sediment and when the value is gradually increased after a certain point the motion of the particles are visible. The circumstances of the flow due to which there is movement in the sediment is called the critical motion. And the shear stress for which there is the movement in the bed it is called as critical shear stress which is denoted by (τ_c). When there is no movement then $\tau_o < \tau_c$. And movement occurs only when the bed shear stress reaches the critical point that is $\tau_o = \tau_c$.

Considering all the available factors likes flow pattern, fluid flow, sediment properties Shields proposed two non- dimensional for the initiation of the motion of the sediment. And these two numbers are Shear Reynolds number and non-dimensional shear stress[22] which can be expressed in equation like

$$R_{*c} = \frac{u_{*c}\, d}{v} \quad \text{(Shear Reynolds number) …...…(2)}$$

$$\tau_{*c} = \frac{\tau_c}{(\Upsilon_s - \Upsilon)\mathrm{d}} \quad \text{(Non-dimensional shear stress)…(3)}$$

Where, d = diameter of the bed particle

$\Upsilon_s = \rho_s g$ = unit weight of the sediment particle

$\Upsilon = \rho g$ =unit weight of water

τ_c = critical shear stress

$u_{*c} = \sqrt{\frac{\tau_c}{\rho}}$ = shear velocity at the critical condition

ν = kinematic viscosity of water

From the several experimental analysis Shields finds a functional relationship between these two parameters $R_{*c}\ and\ \tau_{*c}$. And the curve which represents this relationship between these two is known as Shields Diagram. The shield diagram is given in the next page.

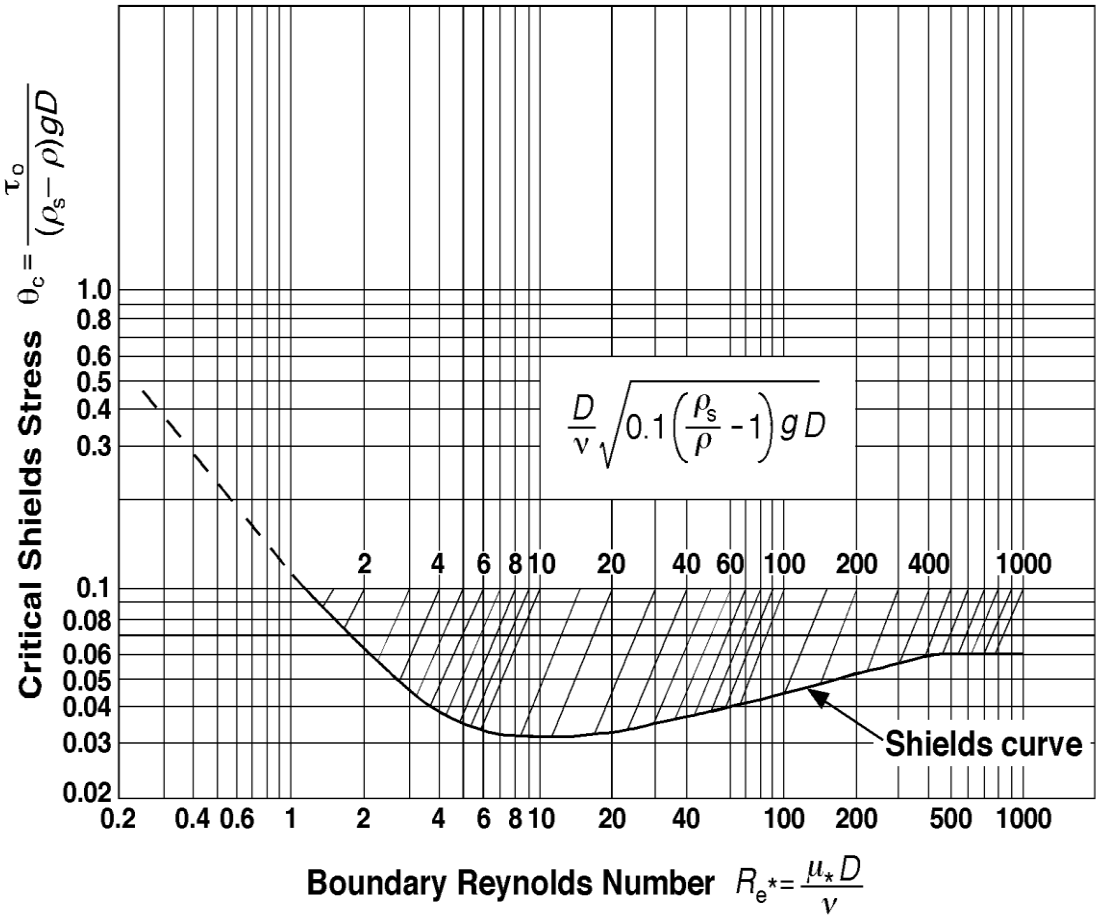

Figure 3: Shield diagram/curve[22]

From the Shields curve it is very clear that up to R_{*c} = 2 the flow is pretty much smooth in nature and particle diameter doesn't have any effect on the critical shields stress. For 2< R_{*c} < 400 there has a transition stage and both the velocity and particle diameter has effect on critical shields stress and after that range it became nearly constant. As the size of the sediment is non uniform in nature so it is convenient to take median size (d_{50}).

Sediment load is another important parameter in case of measuring the transportation or movement of sediment and which generally defines as the combination of both Bed Load and Suspended Load.

2.2 Scour and its classification:

It is a general phenomenon occurs due to the flow of water where sediment is being moved. Scour generally influences by the effects of abutments and piers when water passes across these structures and a net change in the bed elevation is observed. When the bed elevation decreases due to the erosion of bed then it is called as degradation where the increase of bed elevation due to the deposition of sediment is called as aggradation. Scouring can be divided into three main types which are:

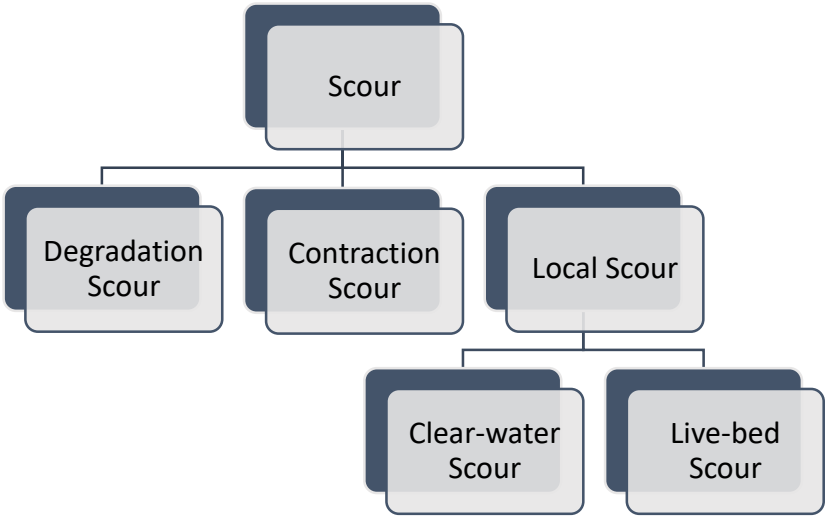

Figure 4: Classification of scour

i. **Degradation Scour**: The long term process which causes the lowering of the sediment bed for the flow of water and which is may not be evident after passing of the flood event.

ii. **Contraction Scour:** Which occurs due to the contraction of the flow passage area of the water naturally or due to other obstructions and result increasing velocity in the water flow. It is commonly termed as general scour.

iii. **Local Scour:** This type of scour happening due to the abutments and piers which create vortex around the hydrodynamic structure and take the sediment away from the structure making it very weak and unsafe. The same amount of sediment that is being moved from the piers is transported to another position.

Local scour are two types:

a) **Clear-water Scour:** It refers to the condition where there is no sediment movement thus no sediment is being transported to the scour prone zone due to this type of scour.

b) **Live-bed Scour:** Here sediment is transported with water in the flowing direction and which led the decrease in the height of the scour. For this type of scouring it takes some time to reach equilibrium condition. The depth of the scour will oscillate about a mean position.

All these above three types of scour like degradation, contraction and local scour together define the scouring around the bridge piers.

2.3 Scouring mechanism:

The maximum failures of bridges occur for the scouring which removes the sediment from the base of piers. And researches are being carried out across the world to make the pier design safe and economical. When water is flowing toward the pier there creates a stagnation point at the intersection between the pier and the direction of the flow where velocity comes to complete rest. The velocity distribution of the approaching flow varies from zero at the bed surface up to the maximum at the surface of water that creates a pressure gradient from the bottom to the top. This change in pressure creates vortex at the bottom of the pillar that sweeps sediment from the region and the vortex looks like a horse shoe. For that reason, this type of vortex is called horse shoe vortex.

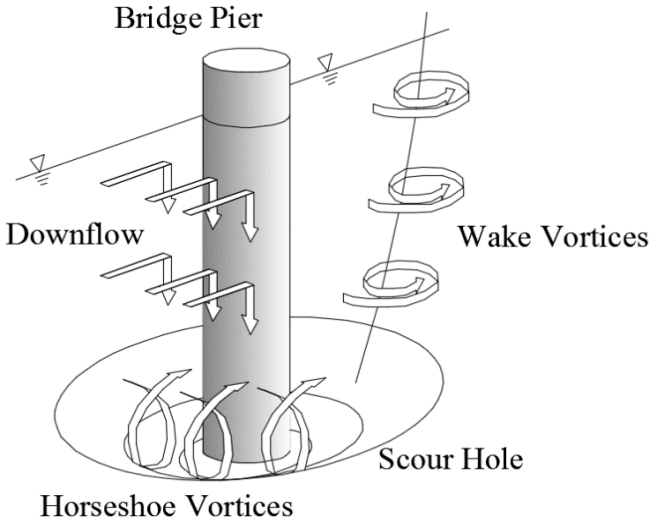

Figure 5: Scouring mechanism due to horse shoe vortex system(THSV)[24]

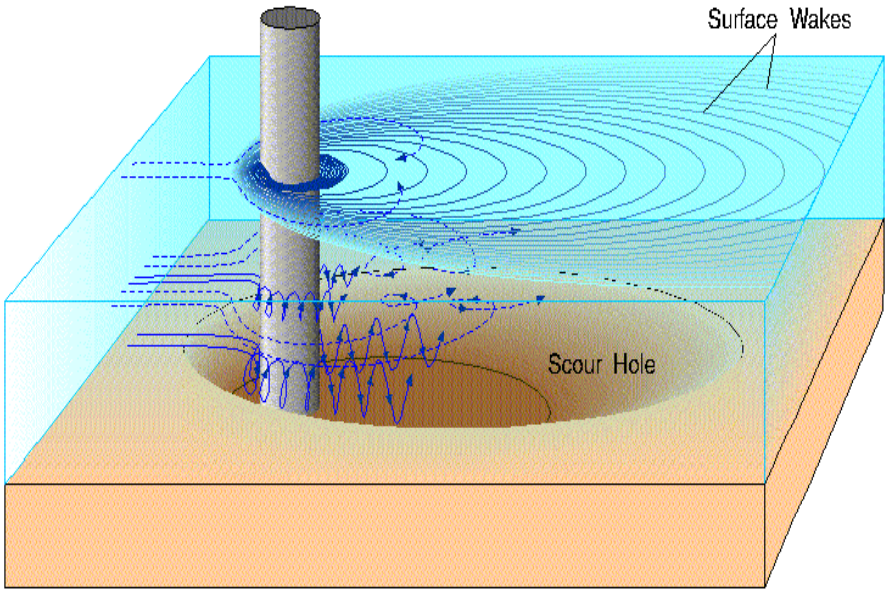

Figure 6: Horse shoe and wake vortices around a cylindrical element[23]

It is the most prominent reason for the scouring. Another type of vortex occurs at the separating reason behind the pier called as wake vortex. Sediment are transported from the horse shoe vortex region and taken outside of the wake vortices region which creates scour around the piers. In case of Live-bed condition the amount of sediment going out of the pillar region is much higher than the amount of sediment coming into the region. And gradually due to the development of scour hole the strength of the horse shoe vortex diminishes for that reason amount of sediment going out is being reduced. That guides to the equilibrium condition and development of hole ceases. In Clear-water condition when the shear stress equals the critical shear stress of the sediment particle then the scour development ceases.

2.4 Factors affecting bridge scour:

Local scour and General scour are very much affected by some important factors and these factors has been discussed by (Melville and Coleman, 2000)[24]

i. **Flow parameters:** Which include the approach flow velocity, the angle of contact between the flowing fluid and the structural geometry. It also includes water transport, sediment transport and debris transport. Approach flow depth is a very important factor which influences the pressure gradient

between the uppermost surface and the sediment bed that excavate the scouring process.

ii. **Fluid property:** The property of any fluid has been characterized by its density (ρ) and viscosity (ν). And these parameters are sensitive to the temperature change. In the normal laboratory study or numerical analysis, we take these as constant at a definite ambient temperature which is not the case in real world where the temperature of the atmosphere is changing continuously.

iii. **Geometrical factors:** Shape and structure of the pier has an imperative impact on the scouring issue. Because it determines the degree of constriction that has been made by the structure on the path of the flow. It made the water passage area relatively smaller and that influences scouring.

iv. **Time:** Reaching into equilibrium condition there need some time and enough time should be provided for equilibrium condition to be exist. In case of numerical analysis time should be set so as to ensure that flow reaches equilibrium conditions as well as the scour depth.

v. **Sediment properties**: Here two conditions exist like live bed scour and clear water scour. And it can't be predicted by observation. In case of live bed scour sediment are transported with water where in clear bed scour sediment are not transported with water. Other than these, particle size, distribution for non-cohesive sediments, spatial distribution of sediment size are important factors.

Chapter 3 Numerical Methodology

Here the numerical analysis of scouring around bridge piers of different structural geometry will be simulated and analyzed further. A comparative study of scour depth as well as other parameters among these structures will be put in front for a relative judgment.

3.1 Governing equations:

In this work FLOW-3D has been used for simulation purpose. Where it has been fully coupled with fluid flow, allows multiple non-cohesive species and considers entrainment, deposition, bed load transport and suspended load transport. Volume and area fraction that describe the packed sediment are calculated throughout the whole domain at each and every time step that is being incorporated by the user. Bed shear stress, the critical shield parameter, erosion rate, bed load transport rate etc. are calculated at each mesh cells of the sediment bed for the better prediction in sediment scouring process. Bed shear stress is calculated using standard wall function that consider the bed surface roughness which is related to the median grain size d_{50} . The sediment scour model undertakes several sediment types with diverse properties including grain size, mass density, critical shear stress, angle of repose and parameters for entrainment and conveyance. The model is used to calculate bed load transport, suspended load transport, sediment transport process, entrainment as well as deposition of sediment. Where entrainment is the process that move the sediment from the packed bed surface and moved to other site. This phenomenon can be only seen when the bed shear stress exceeds critical value of the shear stress. On the other hand, deposition is the process where sediment from the outside area come into the packed bed region due to the effects of various factors like friction, gravity, buoyancy effect. And bed load means the particles in the flowing fluid that are transported along with the bed. Bed load movement means the movement of bed load by rolling, sliding and saltating.

3.1.1 Bed shear stress: It is a shear stress that is stuck on the bed and measured by wall function for 3D turbulence flows,

$$u = u_\tau \left[\frac{1}{k}\ln\left(\frac{Y}{\frac{\nu}{u_\tau}+k_s}\right)\right] [25] \ \ldots\ldots \ \ldots\ldots..(4)$$

Where, u_τ = the shear velocity, $u_\tau = \sqrt{\frac{\tau}{\rho}}$, τ= bed shear stress and ρ=bulk density of the fluid-sediment mixture,

Y= distance from the wall,

ν = kinematic viscosity of the bulk flow,

K= 0.4 is the Von Karman Constant and k_s is related to the grain size and can be defined as

$$k_s = C_s d_{50} \ldots\ldots\ldots\ldots\ldots\ldots..(5)$$

d_{50} = Median grain diameter of the bed material,

C_s = user defined coefficient, usually recommended value is 2.5.

3.1.2 Critical shields parameter: It is a dimensionless form of bed shear stress that can be defined as

$$\Theta_n = \frac{\tau}{g d_n(\rho_n-\rho_f)} \ldots\ldots\ldots\ldots\ldots..(6)$$

Where, g = gravity in absolute value,

ρ_n = the mass density of sediment grains, and

d_n= grain diameter. The subscript n represents the n-th sediment species.

Critical Shields parameter are defined at the critical bed shear stress where there has movement in the bed load that is movement of sediment particle. For both entrainment and bed load transport the equation can be written as

$$\Theta_{cr,n} = \frac{\tau_{cr,n}}{g d_n(\rho_n-\rho_f)} \ldots\ldots\ldots\ldots\ldots..(7)$$

The base value of $\Theta_{cr,n}$ is for a flat and horizontal bed of identically-sized grains. It can be either quantified by users (0.05 by default) or determined from the Soulsby-Whitehouse equation (Soulsby and Whitehouse, 1997),

$$\Theta_{cr,n} = \frac{0.3}{1+1.2\ d_{*,n}} + 0.055(1 - e^{-0.02\ d_{*,n}}) \ldots..(8)$$

And here $d_{*,n}$ is dimensionless grain size, written as

$$d_{*,n} = d_n \left[\frac{g(S_n-1)}{\nu_f{}^2}\right]\text{……..……(9)}$$

Here, $S_n = \frac{\rho_n}{\rho_f}$ and ν_f = kinematic viscosity of the fluid.

3.1.3 Entrainment and deposition: These two are considered as exactly opposing micro processes that occur during the same time. The combined effect of these two are calculated for the net rate of exchange between suspended and packed sediment. Entrainment is to draw something into its own parameter. During entrainment the velocity at which the sediment leave the packed bed is called lifting velocity. And this velocity can be calculated by Winterwerp et al. (1992),

$$u_{lift,n} = n_b \alpha_n d_{*,n}^{0.3} \left(\Theta_n - \Theta_{cr,n}\right)^{1.5} \sqrt{g d_n (S_n - 1)}\text{……(10)}$$

Where, α_n is the entrainment coefficient of species *n* (default value is 0.018), and n_b is the outward normal vector of the packed bed surface. In deposition, the settling velocity of Soulsby (1997) is used,

$$u_{settle,n} = \frac{g}{g}\left[(10.36^2 + 10.49\, d_{*,n}^3)^{\frac{1}{2}} - 10.36\right]^{\frac{\nu_f}{d_n}}\text{…….(11)}$$

Where g is the gravitational acceleration and $u_{settle,n}$ is in the same direction of the gravitational acceleration.

3.1.4 Bed load transport: The dimensionless bed load transport parameter can be defined by the equation

$$\Phi_n = \frac{q_{b,n}}{\left[g(S_n-1)d_n^3\right]^{\frac{1}{2}}}\text{ ……..……(12)}$$

Where, $q_{b,n}$ is the volumetric bedload transport rate per unit bed width (in units of volume per width per time). Φ_n is calculated using the Meyer-Peter and Muller equation (1948),

$$\Phi_n = B_n(\Theta_n - \Theta_{cr,n})^{1.5} C_{b,n} \ldots\ldots\ldots\ldots\ldots\ldots\ldots(13)$$

Where B_n is the bed load coefficient. It is generally 5.0 to 5.7 for low transport, around 8.0 for intermediate transport, and up to 13.0 for very high transport. For the FLOW-3D the value assigned for bed load transport is 8.0 and which is the most common value found from the analysis of literature. $And\ C_{b,n}$is the volume fraction of species *n* in the bed material which can be expressed as the ratio like,

$$C_{b,n} = \frac{net\ volume\ of\ n\ species}{net\ volume\ of\ all\ species} \quad \ldots\ldots\ldots\ldots\ldots\ldots\ldots\ldots\ldots(14)$$

And satisfies

$$\sum_{n=1}^{N} C_{b,n} = 1.0 \ldots\ldots\ldots\ldots\ldots\ldots\ldots\ldots\ldots\ldots\ldots(15)$$

Here, N is for the total number of species. $C_{b,n}$ doesnot exist in the original Meyer-Peter and Muller equation. It is added in equation to account for the effect of multiple species.

The relationship in Van Rijn (1984) is used to estimate the bed load layer thickness h_n,

$$h_n = 0.3 d_n d_{*,n}^{0.7} \left(\frac{\Theta_n}{\Theta_{cr,n}} - 1\right)^{0.5} \ldots\ldots\ldots\ldots\ldots\ldots(16)$$

And the bed load velocity is

$$u_{b,n} = \frac{q_{b,n}}{h_n C_{b,n} f_b} \quad \ldots\ldots\ldots\ldots\ldots\ldots\ldots\ldots(17)$$

Here f_b is the total packing fraction of sediment. And $u_{b,n}\ and\ q_{b,n}$ are in the identical direction of fluid stream adjacent to the bed interface.

3.1.5 Suspended load transport: Suspended sediment concentration can be calculated by solving the transport equation of each species.

$$\frac{\partial C_{s,n}}{\partial t} + \nabla.\left(C_{s,n}u_{s,n}\right) = \nabla.\nabla(DC_{s,n}) \text{ ……...…...……(18)}$$

Here $C_{s,n}$ is the suspended sediment mass concentration, which is defined as the sediment mass per volume of fluid-sediment combination; *D* is the diffusivity; $u_{s,n}$ is the sediment velocity of species *n*. It is noted that each sediment species in suspension moves at its own velocity that is different from those of fluid and other species. This is because grains with different mass density and sizes have different inertia and get dissimilar drag force.

$C_{s,n}$, suspended sediment mass concentration can be defined as the suspended sediment species *n* volume per volume of fluid-sediment mixture. And it can be related to $C_{s,n}$ by

$$c_{s,n} = \frac{C_{s,n}}{\rho_n} \text{……(19)}$$

The mass density of fluid sediment mixture can be calculated using the equation,

$$\bar{\rho} = \sum_{m=1}^{N} c_{s,m}\,\rho_{s,m} + (1 - c_{s,tot})\rho_f \text{……(20)}$$

Where $c_{s,tot}$ is the total suspended sediment volume concentration,

$$c_{s,tot} = \sum_{m=1}^{N} c_{s,m} \text{……(21)}$$

And the help of these equation the main suspended load transportation equation can be solve in FLOW-3D.

3.2 Turbulence modelling:

It is a way of construction and use of a mathematical model for the prediction of effect of turbulence in fluid flows. Turbulence consists of high frequency fluctuations and formation of different varieties of eddies with energy variation. It's a very complex

process in fluid and that depends on various causes like dynamic structure, flow area, approach flow velocity and others Turbulence is mainly characterized by Reynolds number. High value of Reynolds number makes the flow turbulent in nature and in most of the scenario we are encountered with turbulent flow. There has a number of way of turbulence modelling and in this analysis we have used Renormalized Group (RNG) turbulence modelling which is the simplest and the most effective method of establishing scaling of specific models and calculating the corresponding critical exponents. The Renormalized Group (RNG) k-ε model (Yakhot & Orszag 1986, Yakhot & Smith 1992) is a more robust version of the two-equation k-ε model, and is suggested for most industrial problems. It extends the capabilities of the standard k-ε model to provide better coverage of transitionally-turbulent flows, curving flows, wall heat transfer, and mass transfer and which has been mainly developed for the Navier Stokes equation for the energy dissipation rate and kinetic energy.

The renormalization group is useful to derive a nonlinear algebraic Reynolds stress model of turbulence in which the Reynolds stresses are quadratic functions of the mean velocity gradients. The objective of the renormalization group analysis is a theory of the large scales of turbulence in which the effects of small-scale fluctuations are described by an effective or renormalized coupling constant and viscosity. In Renormalizes Group modelling application of low Reynolds number in systematically deriving the theory is a great advantage. And which is especially vital for the square duct where the secondary flows are starred at low Reynolds number.The renormalization group theory cannot be utilized to viscosity dominated flow regions alike the viscous sub layer of a turbulent boundary layer because the primarily viscous scales of motion are removed by the ultraviolet cutoff of the renormalization group procedure. Accordingly, new hypotheses are essential to compute the flow in the viscous region.

The Yakhot-Orszag renormalization group has been developed to solve non-linear turbulence equations and that has been done by evaluation of Reynolds stresses of second order in the Ɛ expansion of the Yakhot-Orszag theory. And because of its converging nature for different turbulent models it has been used for the analysis of scouring process in this paper.

3.3 Numerical modelling of bed:

In this analysis we have numerically studied on the turbulent flow over the open channel bed with a vertical pillar mounted on the bed and which has been located 4m downstream of the inlet region of water flow. This study has been dealt with a total number of five geometric structures of pillars which are a circular pier, square shaped pier, diamond shaped pier, hexagonal shaped pier(new case study) and an airfoil shaped pier(new case study). In the case of circular pier, the diameter has been taken as 16.51 cm. For square shaped pier, each edge length is 16.51cm and for diamond shaped pier, width is 23.35 cm. The related dimension of circular, square and diamond piers are taken from the experiment of Ali Khosronejad & Seokkoo (2012)[26]. Considering the hydraulic diameter of previous three shapes, we determined the edge length of 10 cm for hexagonal shape. The distance between two edge is 50 cm (around 3 times of diameter) & diameter is 17 cm for the airfoil one. The total length of the bed is 10m long and has a rectangular cross-section which is 1.21m wide and 45cm deep. And the flume has a 20 cm layer of uniformly graded non-cohesive sand with a mean particle diameter of $d_{50} = 0.85mm$[26]. All the surfaces including the sediment bed and the side wall of the fumes are considered as smooth and without any surface roughness.

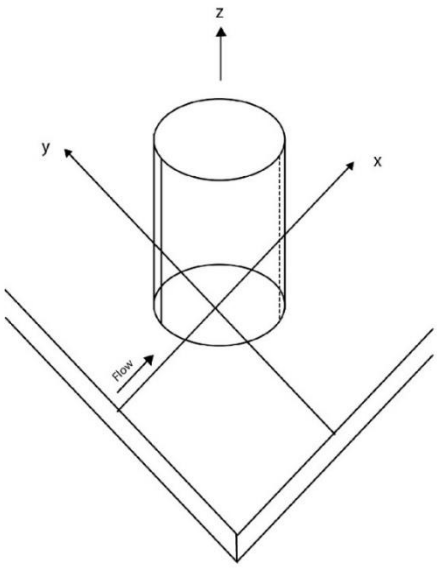

Figure 7: Circular bridge pier geometry

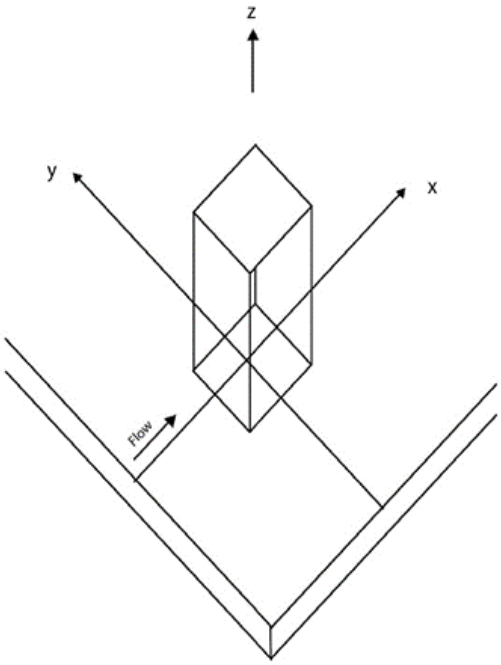

Figure 8: Square bridge pier geometry

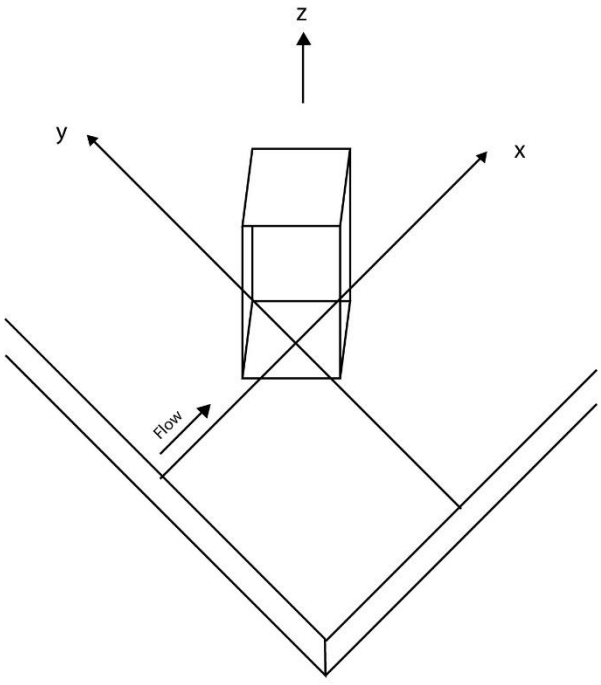

Figure 9:Diamond bridge pier geometry

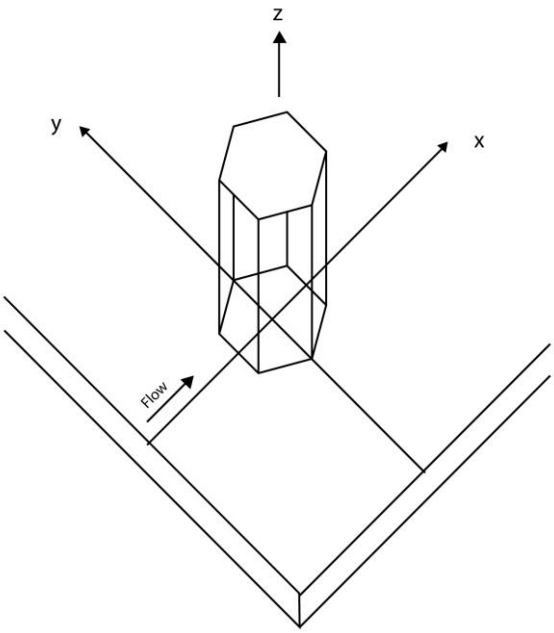

Figure 10:Hexagonal bridge pier geometry

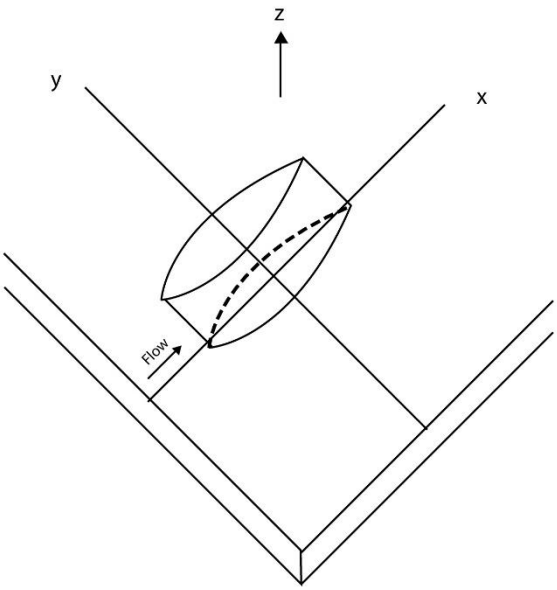

Figure 11:Airfoil bridge pier geometry

Factors for scouring	Dimension
❑ Piers shape ▪ Circular (Diameter) ▪ Square(Edge Length) ▪ Diamond(Edge Length) ▪ Hexagonal(Edge Length) ▪ Airfoil Distance between two edge Diameter	 16.51cm 16.51cm 23.35cm 10.00cm 50.00cm 17.00cm
❑ Bed Structure ▪ Length ▪ Width ▪ Height	 10.00m 1.21m 45.00cm
❑ Flume Height(uniformly graded non-cohesive sand)	20.00cm
❑ Pier Location	4m(Downstream of the inlet region of water flow)

Table 1: Pier geometry and bed structure data and location of pier from inlet

Factors for scouring	Dimension
❑ Mean Particle Diameter (non-cohesive sand)	0.85mm
❑ Critical shield number	0.05
❑ Sand Density	1602 kg/m^3
❑ Turbulence Model	RNG
❑ Fluid	Water at 20 C
❑ Volume Flow rate	0.057 m^3/s

Table 2: Sand properties and used turbulent model

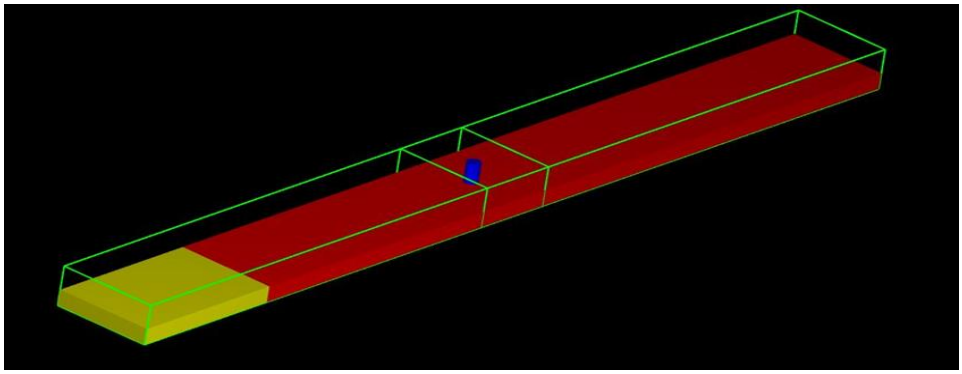

Figure 12:Location of mesh plane at x= 3.5m and x=4.5m from inlet

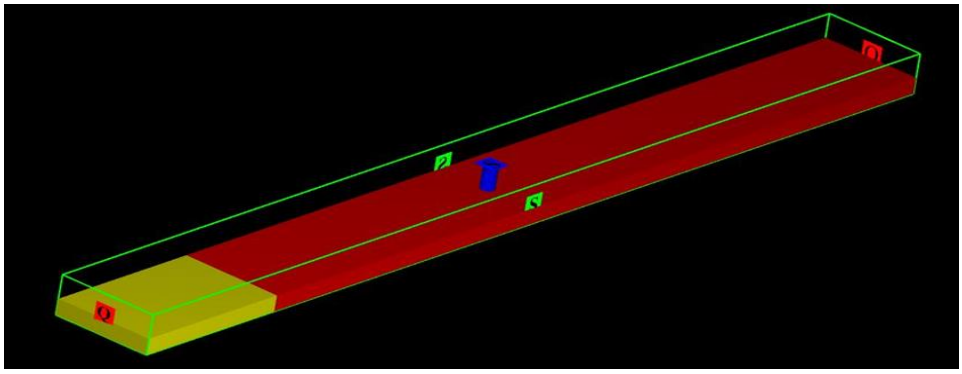

Figure 13: Boundary conditions

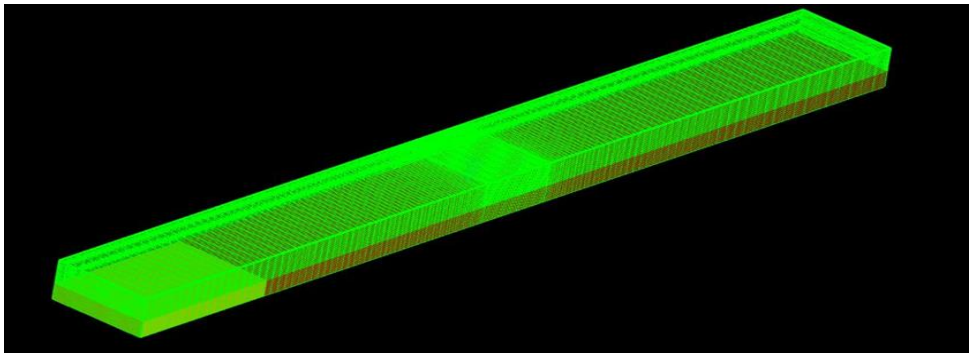

Figure 14: Meshing of geometry

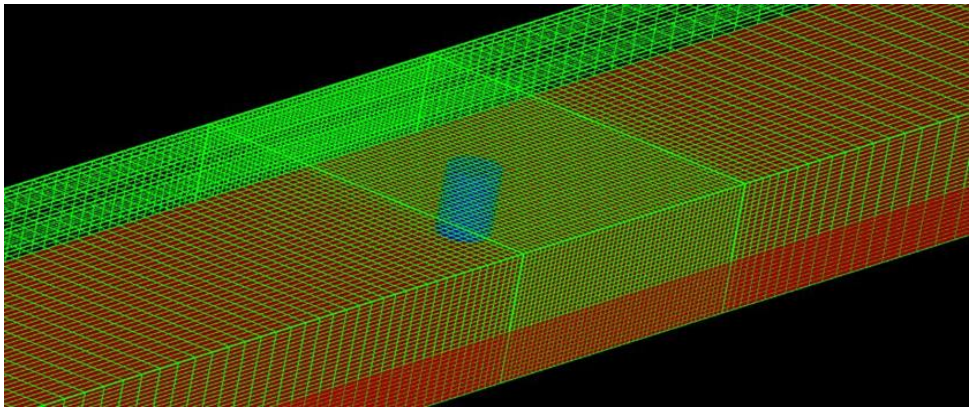

Figure 15:Grid refinement around bridge piers

All of these numerical simulation has been run based on the clear water condition for each of the geometries. At the start of the numerical analysis sediment bed elevation has been recorded and the simulation has been run until equilibrium conditions are reached and the scour depth reaches in equilibrium for each of the case.

For any experimental analysis the equilibrium condition is considered to be reach at the time when the rate of increase of scour depth doesn't exceed 5% of the pier diameter over a period of 12 h [27]. And when these conditions are reached then the flow is terminated and the available depth and scour geometry are taken into account. But in case of numerical study we have observed that flow reaches in equilibrium condition in much rapid pace than it does in case of experimental study. In the numerical simulation we have carried out grid test of varying resolution ranging from 2 lakhs to 3 lakhs to investigate the numerical errors occurred changing the grid resolution. And then we came up with a grid resolution that is better to capture our whole dynamics.

Scour around circular pier, square shaped pier and diamond pier has been studied previously and different aspects of the structure change and its effects and causes has been discussed with their reasons [28,29]. According to our knowledge so far and study upon different sources, we considered our work on two different geometries of pier like hexagonal and airfoil are unique in this field. And we considered these two as our topic of interest because their edges and in airfoil, the water stream supposed to move in streamline if the flow has a lower Reynolds number and these have small effects on the scour depth. In this paper we have numerically studied on these two structures along with the three above and compared their results for coming to a conclusion.

Now we will at first discuss various computational details and at the same time we will present the results for each of the cases.

3.4 Grid test:

Grid independency has been carried out in case of circular pier. Where the rectangular structured mesh are ranging over the sediment bed and the pillar. A number of cells has been defined to discretize the governing equations. The resolution of the grid has changed from the coarser one to the finer one to get acquainted with the effect of structured grid over the numerical result. FLOW-3D is dealing with the structured rectangular mesh and for that reason it is implemented on our overall structure.

We have carried out three grid test on circular pier which are A (coarsest), B (not so coarse and not so fine), C (finest). For all of these extra mesh planes has been added around the pier (one plane 3.5m from the upstream and another one 4.5m) to get and capture the scouring depth very precisely and for better results. Then the results are analyzed for coming to a conclusion. The details of the various computational grids, including the number are shown below:

Grid	Number of grid nodes	Total number of cells
A	$333 \times 30 \times 20$	200000
B	$166 \times 50 \times 30$	250000
C	$200 \times 50 \times 30$	300000

Table 3: Number of grid nodes in each direction and number of total cells in each grid system

The results on scouring depth for these three different grid cells are represented on below.

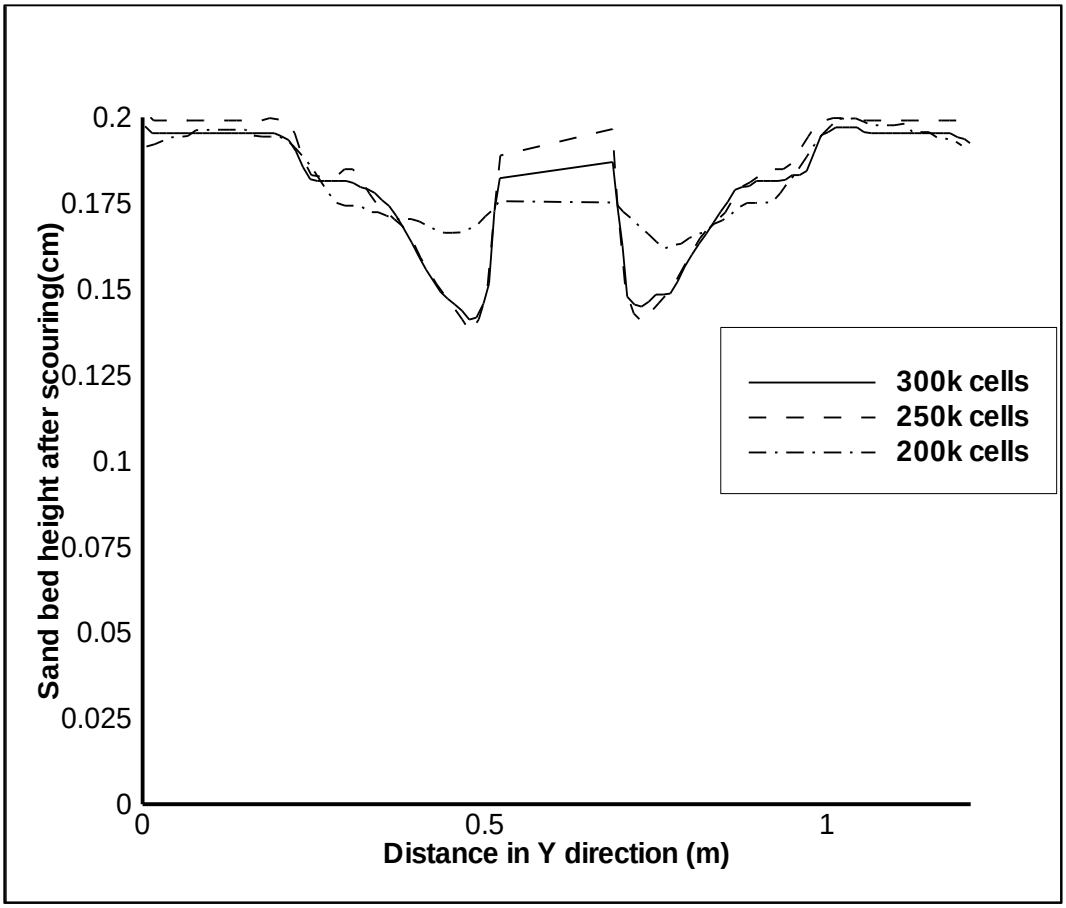

Figure 16: Grid independency test

The above graph illustrates that A (coarsest) with total 200k number of cells cannot predict the scour depth accurately where the results of scour depth for B (with 250k) and C (with 300k) are very close to each other which confirms that grid independency is achieved. So the finest grid C has been taken as a prime one to run the rest of the simulations for other structures. For all these cases time accurate simulations were carried out until it reaches in equilibrium condition.

Chapter 4 Result Analysis

4.1 Comparison of numerical and experimental bed topography at equilibrium:

For any numerical solution, it must have to be validated with respect to the experimental solution. The level of accuracy that prevails in the numerical solution also depends on the predictive capabilities of the software that has been used to run the simulation procedure. Irrespective of the other stuffs results also depend on the number of grids used to define the numerical bed. Here to validate between the numerical and the experimental bed topography, for both of the cases equilibrium time condition has been taken to compare. In the below, numerical topographies of the three geometrical structures e.g. circular, square and diamond shaped piers have been validated with the experimental data available in Ali Khosronejad & Seokkoo (2012) [26]. All negative contour values represent scouring and positive values represent deposition. All numerical values are in cm unit.

4.1.1 The circular shaped pier:

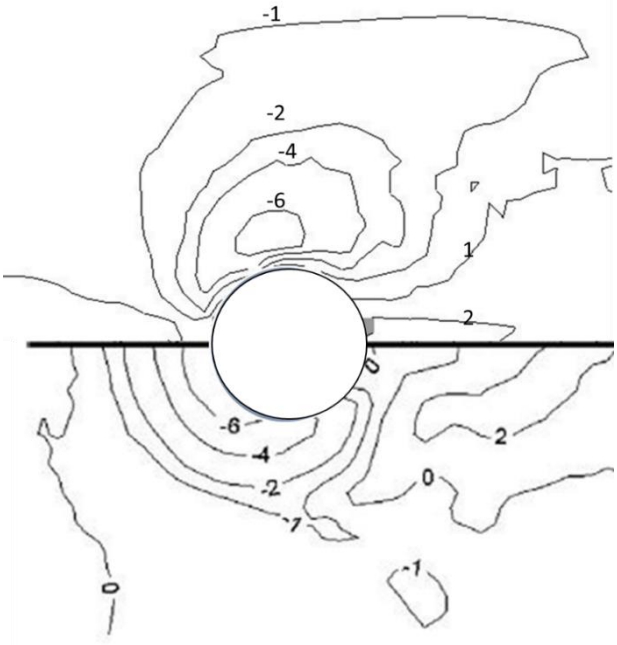

Figure 17:Comparison of experimental (bottom) and numerical (top) bed topography at equilibrium (in cm) for circular shaped pier

When we compare the bed topography of the circular shaped bridge pier, the lower portion of the symmetrical line is the experimental bed topography and the upper portion of the symmetrical line is the numerical bed topography.

In the experimental one it is pretty much clear from the figure that the maximum scour depth occurs from the nose section at the upstream and continuing up to approximately 75 to 80 degrees[26] And scour depth is maximum at the nearest and that gradually decreases when we move far from the pier which eventually at some point turning out to be positive number that indicates that no more sand is removing from that place rather entrainment of sand particles are coming from the other areas. On the other hand for the numerical one the maximum scour depth develops at the side of the pillar and not at the front side of the upstream. And scouring occurs as a small pocket confined at the side of the circular pier. After that scouring gradually decreases when we move far from the centerline of the pillar.

The maximum scour depth that has been observed for the experimental one is 6.7cm[26] and for the numerical one it is 6.5cm. And both of these observed in two different locations where the numerical values for both of the scour depth can be compared with some sacrifice in accuracy.

4.1.2 The square shaped pier:

In the incident of square shaped pier the lower arm of the symmetrical line represents the experimental bed topography and the upper arm of the symmetrical line represents the numerical bed topography. Where in the experimental case study we observed that the maximum scour depth occurs at the upstream front nose of the pier and wraps around the pier and extend up to the side of the pillar. And gradually scouring effect decreases when we reached far from the centerline. At the downstream of the pier section deposition of the sand particles are observed due to the entrainment of the sand particles carrying by the flow itself.

At the time of the numerical bed topography we see the similar type of bed like the circular shaped pier. Where maximum scour depth developed like a small pocket like structure confined at the side of the pillar. And maximum scour doesn't arise at the nose of the square pier. Scouring effect decreases like the previous cases when we go far from the pier. And deposition of sediment particles is observed in the downstream of the pier.

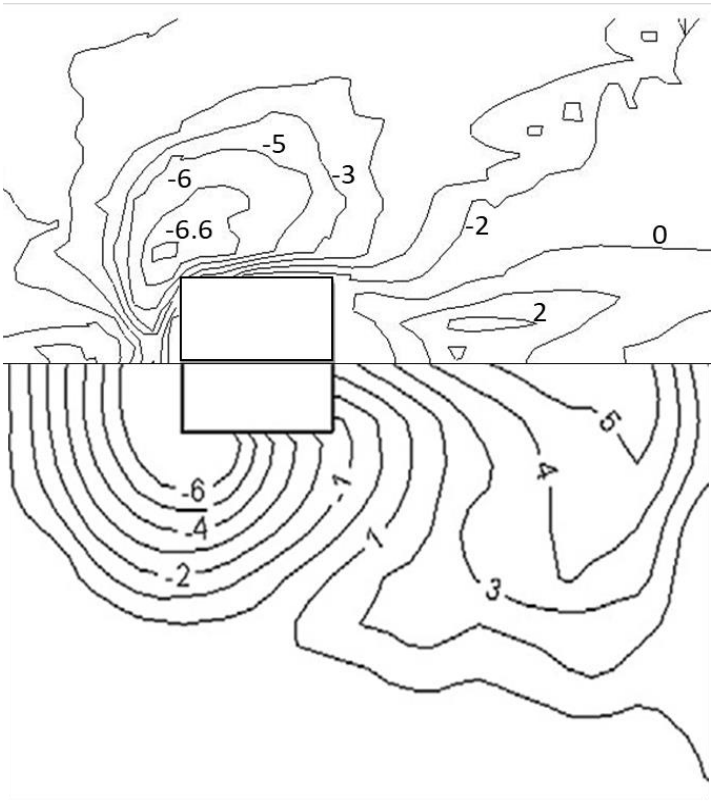

Figure 18:Comparison of experimental (bottom) and numerical (top) bed topography at equilibrium (in cm) for square shaped pier

The maximum experimental scour depth has been recorded as 7.6cm[26] and the numerical scour depth is 6.6cm. The difference between the numerical and the experimental results are much are not satisfactory enough. Because in the real case scouring around square shaped pier has also been influenced by the edges of the pier and that accelerate the scouring mechanism and scouring depth increases but the effect of the edges can't be predicted by the Flow3d software. And for that the scouring depth for those two cases varies a lot.

4.1.3 The diamond shaped pier:

For the above two cases both associated with blunt nose. So for that purpose researchers have introduced diamond shaped pier which is incorporated with edge when comes in contact with the upstream flow of the water. And here significantly a great improvement of the predictive capabilities of the software has been seen. Like the previous times the lower arm represents the experimental bed topography and the upper arm represents the numerical bed topography. For the experimental one the maximum scour develops at the side of the

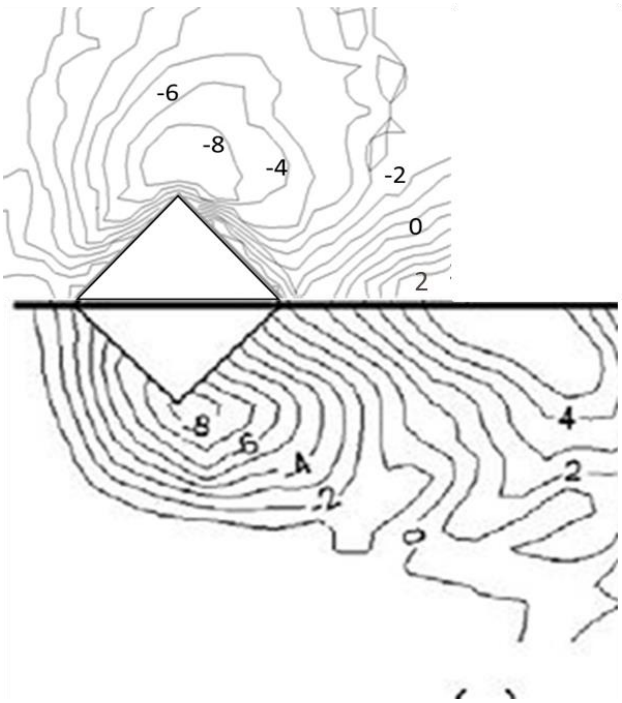

Figure 19:Comparison of experimental (bottom) and numerical (top) bed topography at equilibrium (in cm) for diamond shaped pier

pillar as a confined small structure of pocket and gradually the scouring effect decreases. At the same time if we look at the numerical bed topography we can see the same type of confined small pocket at the side of the pillar which gradually decreases when we move a distance from the center line.

Maximum scour depth at the experimental case is 8.3cm[26] and the numerical one is the 8.5cm. So these two values can be compared very easily and here we get a better result.

From the above analysis we can came to a conclusion that for both the bed topography and numerical values the predictive capabilities of the software Flow 3d depends on the structure of the pier. And in case of the blunt lose the bed topography is not much satisfactory. But for the diamond shape it has a better predictive ability.

The above three structures have been studied by several researchers over the years. Here we would like to investigate two more structures which are the hexagonal shape and airfoil shaped pier and scouring effect associated with these two structures. And according to our study and knowledge these two structures has not been studied yet. The bed topography of these two are enlightened below.

4.1.4 The hexagonal shaped pier:

Here we see that maximum scour develops at the side of the pillar and gradually decreases when we go far from the pillar center. And deposition starts to build up in the downstream of the pier.

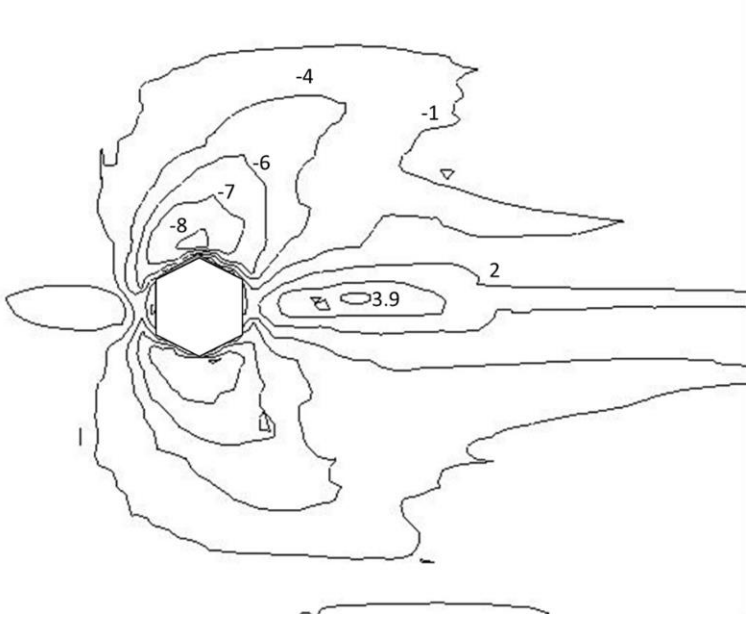

Figure 20:Comparison of experimental (bottom) and numerical (top) bed topography at equilibrium (in cm) for hexagonal shaped pier

The maximum scour depth for the numerical one is recorded as 8.0cm and deposition of sand is recorded as 3.9cm. Maximum scouring occurs as a small pocket at the both sides.

4.1.5 The airfoil shaped pier:

Airfoil shape is one of our interest of study because of its streamlining structure. And here maximum scour develops at the both side of the pillar and forming a confined comparatively bigger pocket like structure.

The maximum scour depth that has been recorded for the airfoil structure is 7.9 cm and the deposition at the downstream of the pillar is 3.8cm. The scouring gradually decreases from the side of the pillar. And from the maximum scour depth value it is clear that there has no development of scouring in case of air foil structure.

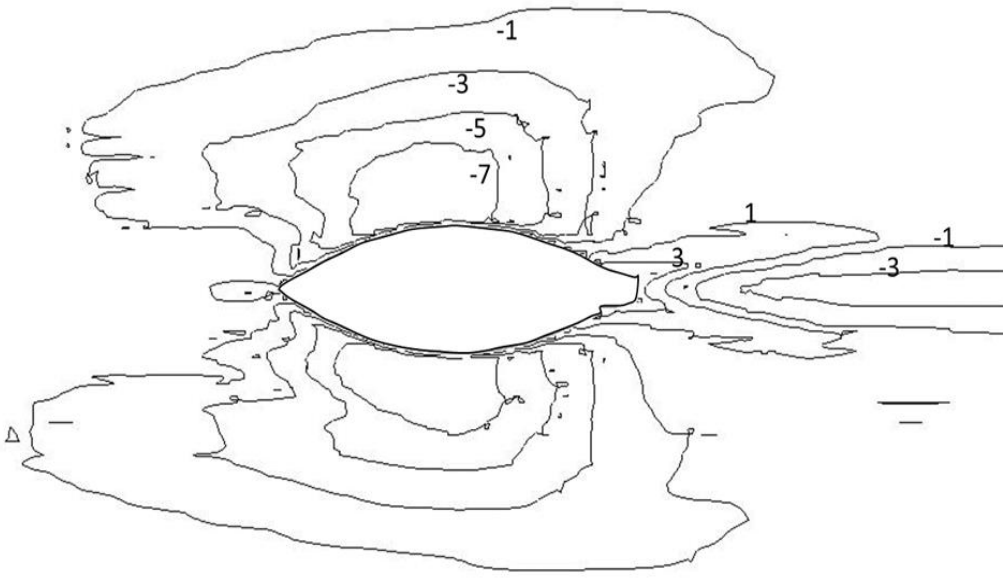

Figure 21:Comparison of experimental (bottom) and numerical (top) bed topography at equilibrium (in cm) for airfoil pier

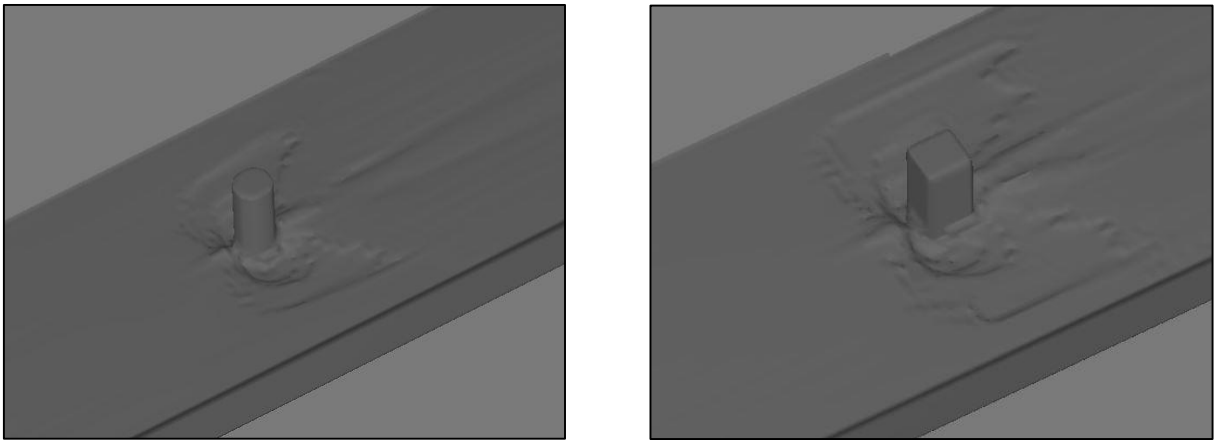

(a) (b)

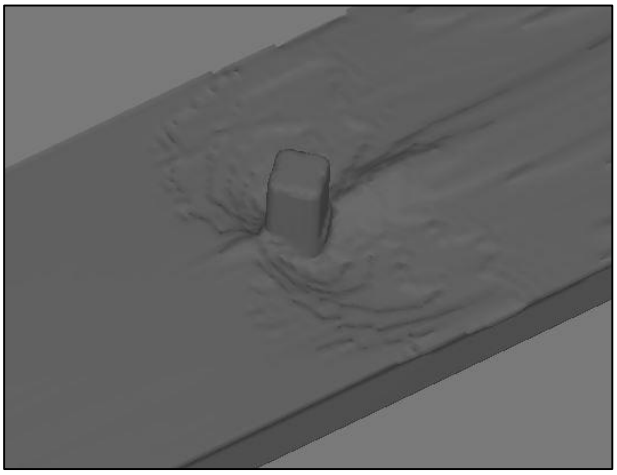

(c)

Figure 22 : scouring depth at equilibrium condition in 3D geometry (a) circular pier (b) square pier and (c) diamond pier

From the above figure, we can observe that the highest maximum scour depth has been found for the diamond shaped pier.

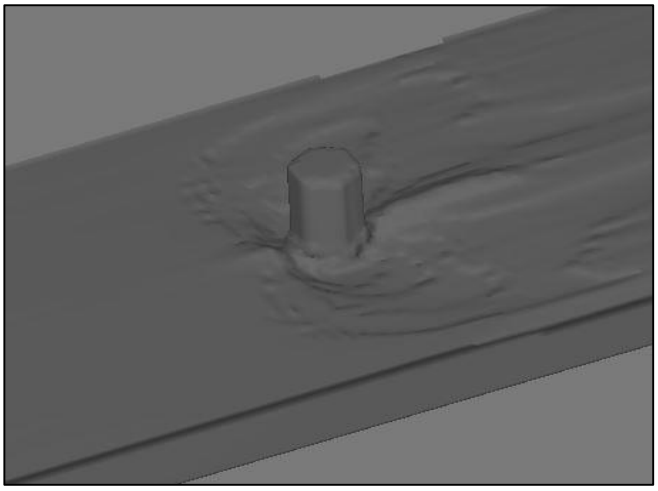

(d)

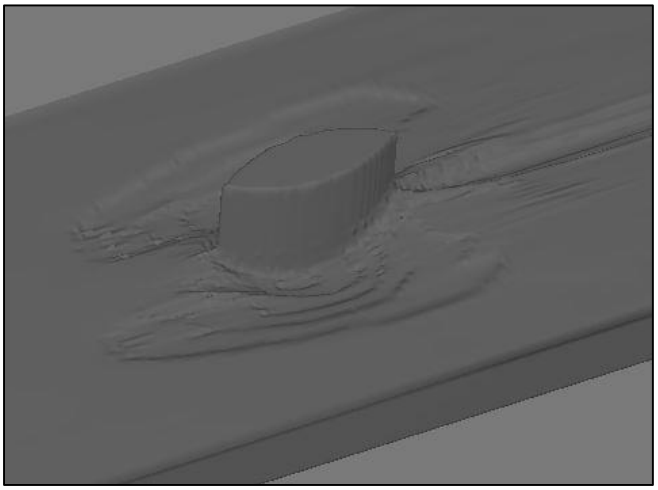

(e)

Figure 23:scouring depth at equilibrium condition in 3D geometry (d) hexagonal pier and (e) airfoil pier

In case of hexagonal and airfoil shaped piers, the maximum scour depth are almost same .

4.2 Validation of scour depth when the time is varied:

From the mechanism of scouring effect, we know that scouring effect increases with respect to the time. At the starting of a water flow across the pier, the velocity remains quite gentle and which has less effect on the scouring process. But when the flow is running for a long time and at the same time the velocity distribution around the pier changes progressively, so it has a consequence on the scouring procedure because at that instant horse shoe vortex system becomes significant. We know that scouring around bridge piers only occur when the approach flow velocity exceeds the critical shear velocity at the critical condition. So for that analysis of scour depth with respect to the time becomes a very important parameter to judge the predictive capability and the other stuffs. And for that consequence here we will try to put up the time dependent scour depth analysis. Experimental data for circular, square and diamond shape are available in Ali Khosronejad & Seokkoo (2012) [26].

4.2.1 The circular shaped pier: In the graph that has been presented below we observe that for the circular shaped pier for the approximately first 300 seconds the shape of the curve of scouring is similar in shape though it has difference in the numerical value.

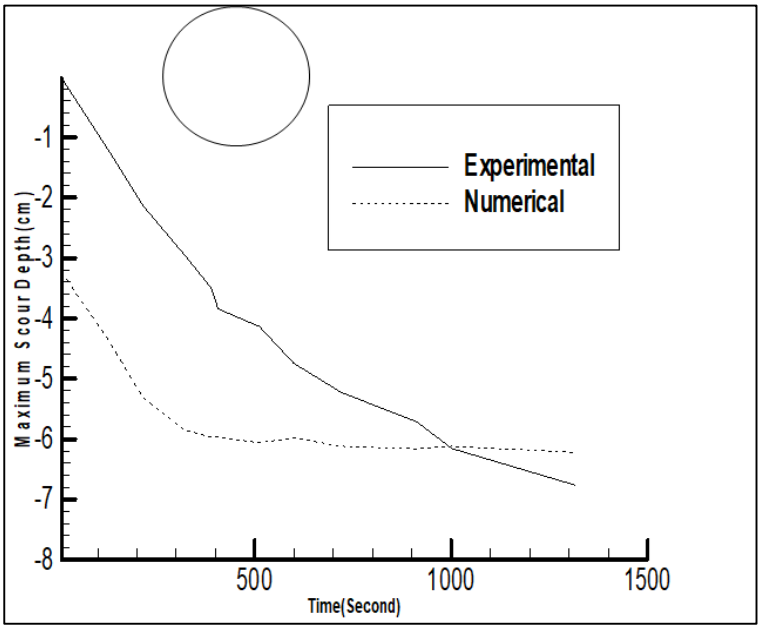

Figure 24: change of maximum scour depth(cm) with time(sec) for both experimental and numerical case for circular pier

But for rest of the time the shape is not the identical in nature. Because from the mechanism of scouring we came to know that scouring occurs only when the velocity surpasses the critical value and that is the reason for scouring in the first few seconds. But for rest of the time scouring also occur due to the generation of horse shoe vortex system along with the velocity effect of water flow. And horse shoe vortex removes sediment particle from the underneath of the structure and that increases the scouring. But we see from the graph that numerical solution can't predict the mechanism of the horse shoe vortex. So it is a limitation for using the software to predict the scouring effect in case of circular pier.

4.2.2 The square shaped pier: Time dependent analysis of the square shaped pier reflects that the irregularities of scouring depth and corresponding curve is more than the circular shaped pier that we have seen before. And here for the first few seconds thought he shape is somewhat similar but not that much. Here also this has been happened because of the scouring mechanism which tells us that when the flow started scouring is only be driven by the velocity where for the later part horse shoe vortex system is also seen.

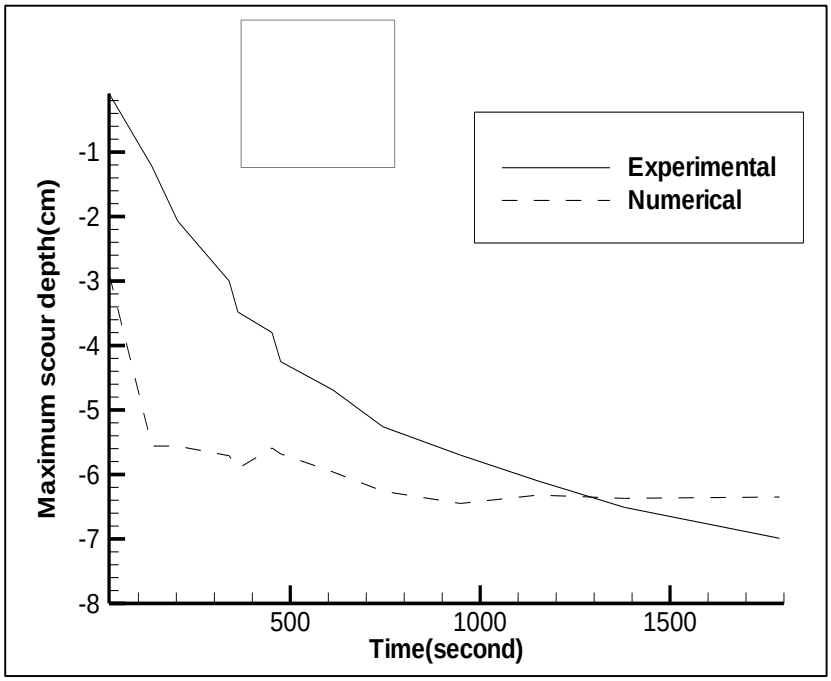

Figure 25:change of maximum scour depth(cm) with time(sec) for both experimental and numerical case for square pier

And from the graph it is clear that scouring is happened at a very first rate for the first few seconds and later on the rate of scouring decreases with the increase in the time of the running of flow of water. Because here the software is not capable enough to capture the scouring that has been occur due to the vortex system and for that reason the curve is not similar.

4.2.3 The diamond shaped pier: Diamond shaped pier is one of the topic of interests because of its nature of geometry which has edge shape pier nose when flow is in the upstream. And due to the presence of the edge, the formation of horse shoe vortex ceases. The edge at the upstream decreases the energy of the horse shoe vortex and that subsequently gives us a better result for the diamond shaped pier.

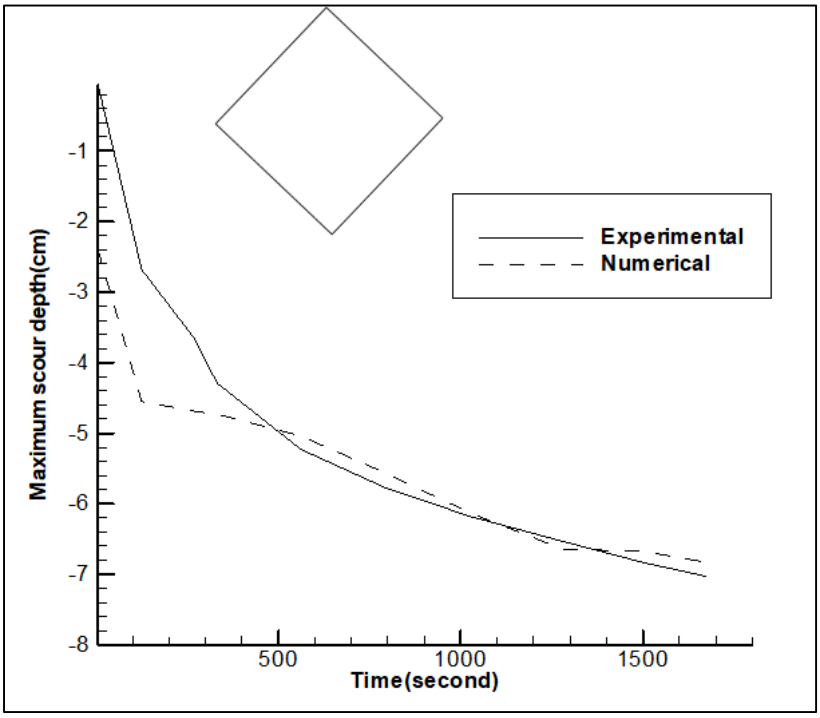

Figure 26:change of maximum scour depth(cm) with time(sec) for both experimental and numerical case for diamond pier

So here from the graph we see that the experimental and the numerical both the curve shape is almost same and also coincide in the values. Here we see a difference between the diamond shaped pier and the rest of the two shapes which are circular and square

one because for the diamond shaped pier the presence of edge at the upstream lower the strength of the vortex that removes sediment from the pier section. And for that in case of scouring around diamond shaped pier horse shoe vortex system isn't an influential factor or a deciding one. So here the wicked predicting capability of the software isn't focused as vortex system isn't playing a vital role.

And for that purpose we have a better time dependent scouring depth curve for diamond shaped pier that the circular and square shaped pier.

4.2.4 The hexagonal shaped pier: This is a new case that has been studied by our research. And in light of the graph that has been presented down below we can explain the time dependent nature of scouring effect of the hexagonal shaped pier. According to the graph for the first 200 seconds the rate of scouring is very fast but for the rest of the simulation the rate gradually decreases with time. Which eventually reaches at an equilibrium. Scouring around hexagonal pier takes a longer time than the others to reach in equilibrium condition.

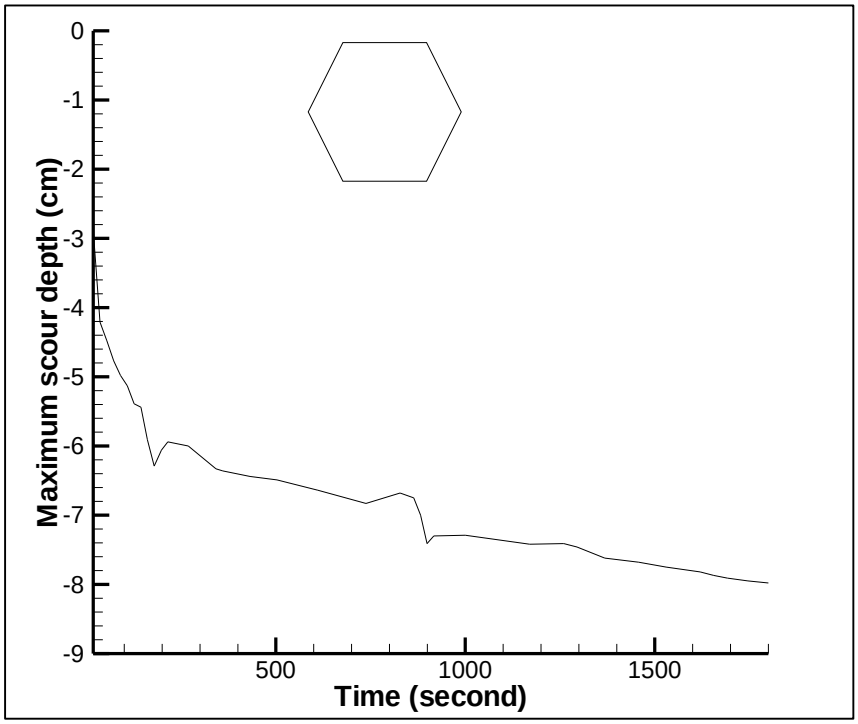

Figure 27:change of maximum scour depth(cm) with time(sec) for both experimental and numerical case for hexagonal pier

4.2.5 The airfoil shaped pier: It is another structure that has been newly introduced by our study to see whether it can give a good result or not. We see from the above graph of the airfoil shaped pier that it reached in equilibrium condition very rapidly and at the first phase of the process the rate of scouring is very fast and then suddenly it dropped drastically. And reached in equilibrium condition. But the scouring is more in the case of air foil shaped pier.

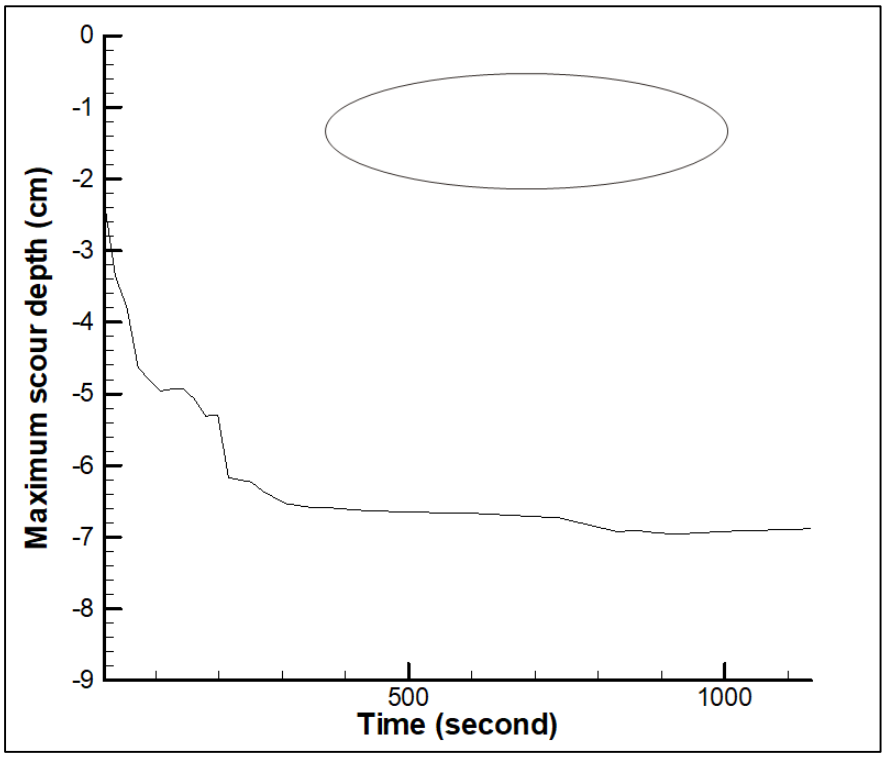

Figure 28: change of maximum scour depth(cm) with time(sec) for both experimental and numerical case for airfoil pier

4.3 Velocity distribution along the flume bed:

Velocity distribution along the bed flume indicates the theory behind the scouring. Here we see that velocity is not constant along the flume bed rather it is different and follows a pattern. According to the contour plot shown below (fig 29) we acknowledge that velocity is highest at the inlet and that is steadily decreasing and came to a complete stop at the pillar and fluid flow interface. And that point is known as stagnation point and here velocity is very less but at the same time pressure increases. From the contour plot another thing is that velocity is also changing along z direction or vertical plane, which is in the order of decreasing. Decreasing of

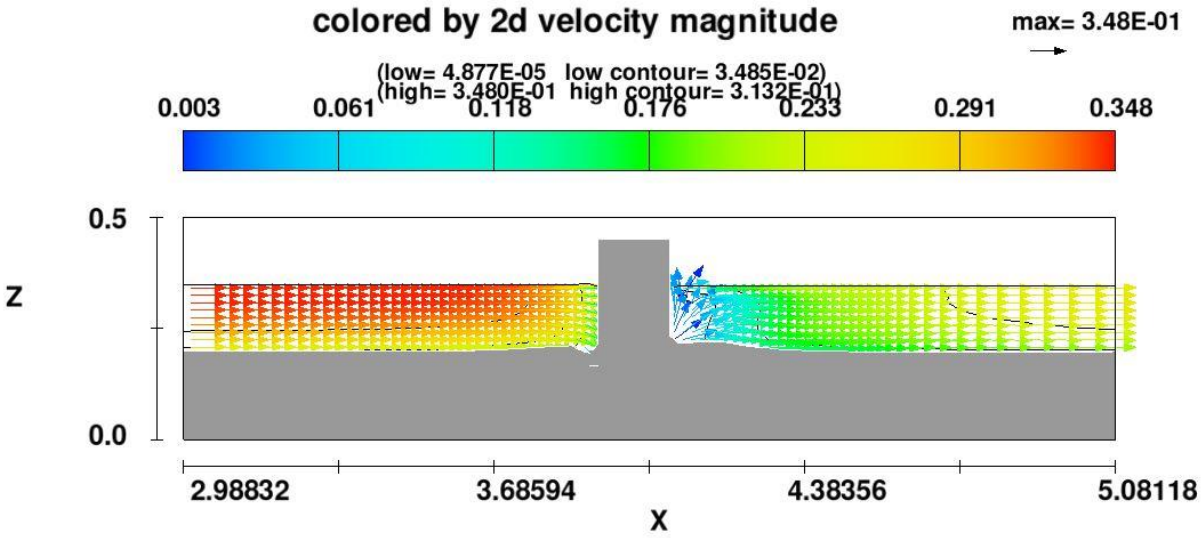

velocity, increases the pressure.

Figure 29: Velocity distribution in xz plane (situated in the middle of the width) for circular pier

So there creates a pressure difference along the vertical direction and that pressure gradient influence the scouring process and removes sediment particle from that region. Scouring is higher in the upstream of the flow at the pillar nose. But if we observe the downstream of the pillar then we see that velocity is lowest at the back of the pillar which subsequently creates a region of unsteady flow and eddy formation of water that is irregular. This region in the downstream of the pillar is called wake region and here wake vortex also form. That creates a scouring region behind the

pillar. As the velocity is very negligible at that region so formation of scour depth is also very small. And beyond the wake region flow again starts to accelerate. Though no scouring is not observed further because there is no abutments or pillar on their flow which could create an obstacle and form local scour.

The above velocity distribution contour (fig 29) is for the circular one and taken at the xz plane. Velocity distribution for rest of the four structures are same and the follow the same principle in the process of scouring.

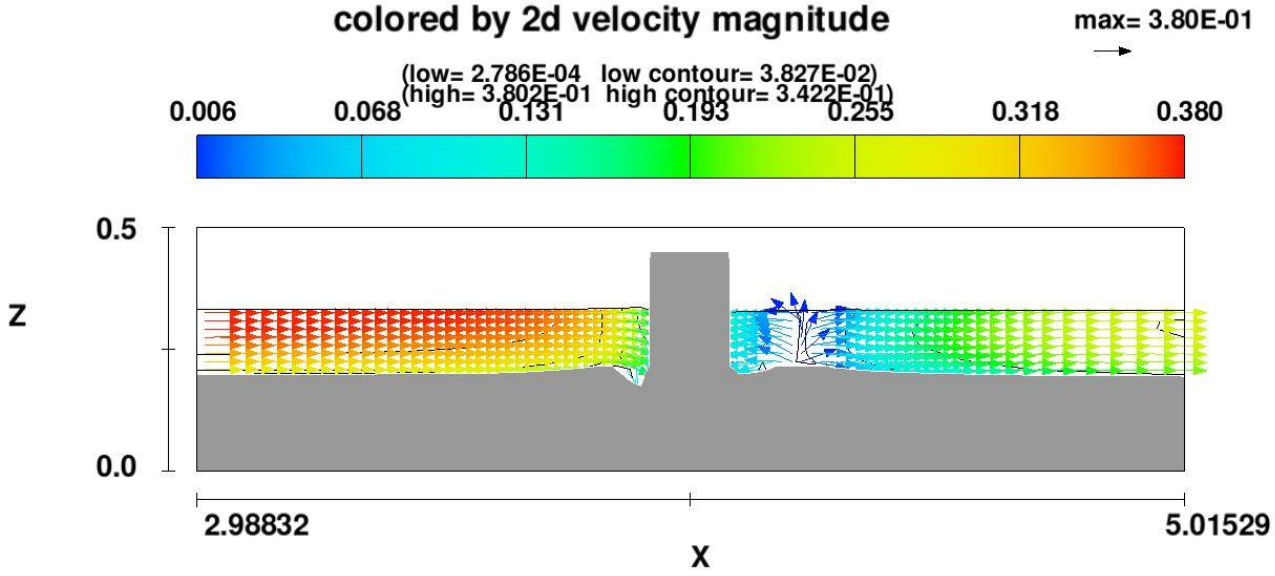

Figure 30: Velocity distribution in xz plane (situated in the middle of the width) for square pier

The above velocity distribution contour is for the square shaped pier. And here we see that vortex region is form at far away from the pier when we compared it with the circular shape. Because in the circular shape due to its circular geometry, flow is much more streamlined but for the square shaped pier flow is not streamlined because of the geometry has edges at the two sides from the center. So the presence of the edges at both upstream and downstream resists the flow to be streamlined. And for that reason formation of wake region is far behind than the circular shaped pier.

Now in case of diamond shaped pier (fig 31) we see that wake region is again close to the pillar. Here in case of diamond flow is again to be gentle and quite streamlined

as the geometry permits to do so. Where in square shape associated with blunt nose but diamond shape pier doesn't associate with blunt nose rather it has sharp nose and also at the downstream the structure of the pillar is sharp. Which is the reason behind the formation of wake region in closer position. Where the other velocity distribution

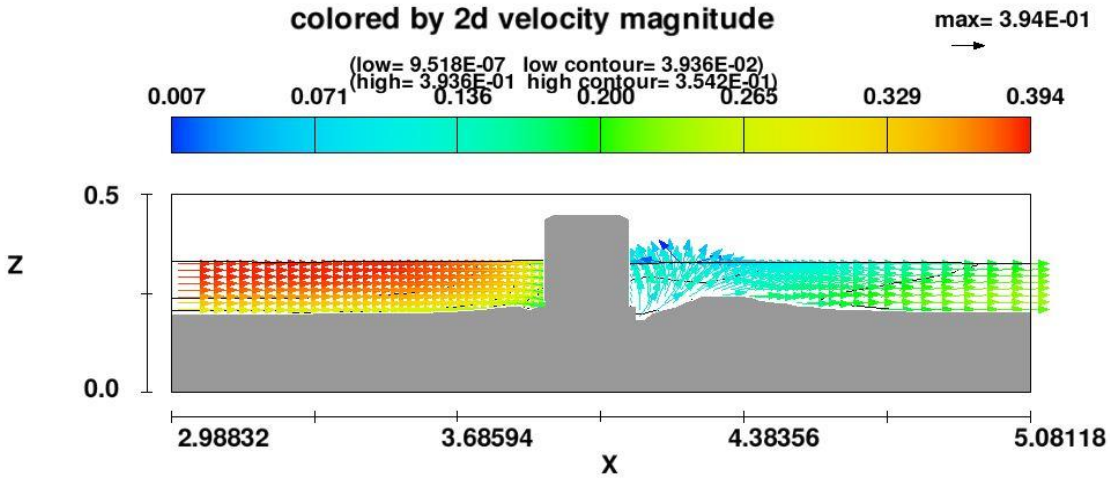

is

Figure 31: Velocity distribution in xz plane (situated in the middle of the width) for diamond pier

same like the previous ones and both of these model follow the same scouring process mechanism to remove the sediment particles from the region of the pillar.

Here down below is the velocity distribution contour plot of hexagonal shaped pier.

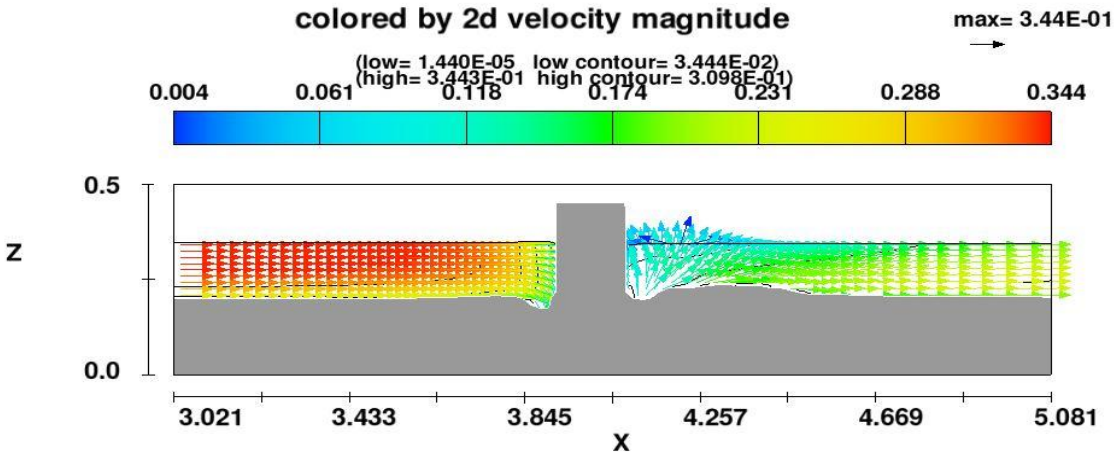

Figure 32: Velocity distribution in xz plane (situated in the middle of the width) for hexagonal pier

And from the contour plot we see that velocity distribution follow the same pattern and that is decreasing from the inlet region of water flow and came to a very negligible value at the pillar and fluid flow interface. And at the back of the pillar wake region has been form. And the direction of the velocity magnitude is outwards in that wake region because here flow is unsteady and eddy formation happens in that region. That irregularities in the flow try to split the fluid along different direction. Without this region other region in the flow has the same direction in nature and which is in the fluid flow direction.

Now for the last case which is air foil shaped pier the velocity distribution contour plot has been presented below.

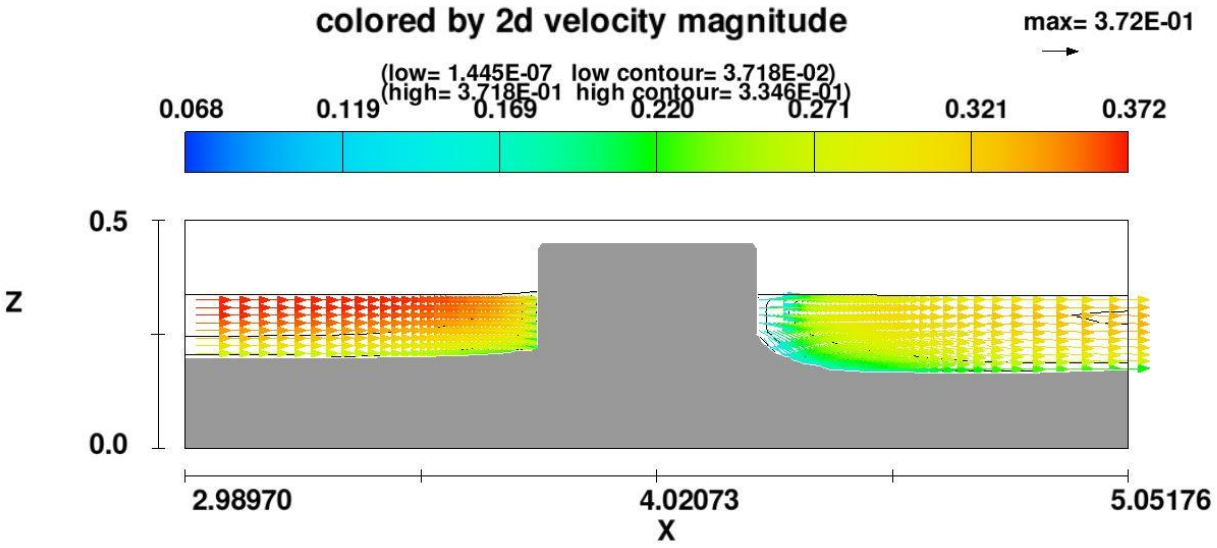

Figure 33: Velocity distribution in xz plane (situated in the middle of the width) for airfoil pier

Where we see that the direction of vector magnitude is not in outward direction like the previous times because here the flow is so streamlined that no irregularities or formation of eddies don't happen. And no significant wake region is there which confirms no formation of wake vortex in airfoil shape structure.

Chapter 5 Summary and Conclusions

In the above we have described the important parameters that effects scouring process and mentioned their causes related to each of these parameters. Scouring is a very common effects that happen around the bridge pier due to presence of abutments or piers and the consequence of that is noteworthy. Scientists around the world working on it for long time to reduce the scouring process. Many structures have been studied and also other techniques have been applied to reduce it but any mentionable progress haven't been yet found that drastically reduce the rate of scouring. In our study we tried to investigate two things. The first thing is whether the software that has been used in our study is capable enough to predict the nature of scouring process which includes both the bed topography and also the maximum scour depth. And the second thing is whether the two new case study models which are hexagonal shaped pier and airfoil shaped pier is good enough to take precedence over the existing models.

From the analysis of the bed topography and time variant scour depth formation we found two very important and noteworthy matters and which are the predictive capabilities of Flow-3d depends on the type of the geometry and another one is in the generation of horse shoe vortex. Where we see in case of blunt nose type geometry structure Flow-3d can't provide good result in terms of bed topography. And at the same time on the other hand for the sharp edge geometrical structure the bed topography has been well defined and captured. Now coming to the second point which is the limitation of Flow-3d in measuring the horse shoe vortex system is still a major drawback of this software. And for that limitation we see in case of the time dependent scouring depth the graph doesn't match for the circular and the square shape, on the other hand in case of diamond we see that both the experimental and numerical curve has similar in their nature because edge in the diamond structure lessening energy contained in horse shoe vortex.

Now if we look at our second purpose of study is to know which structure is more suitable to select as the pillar structure.

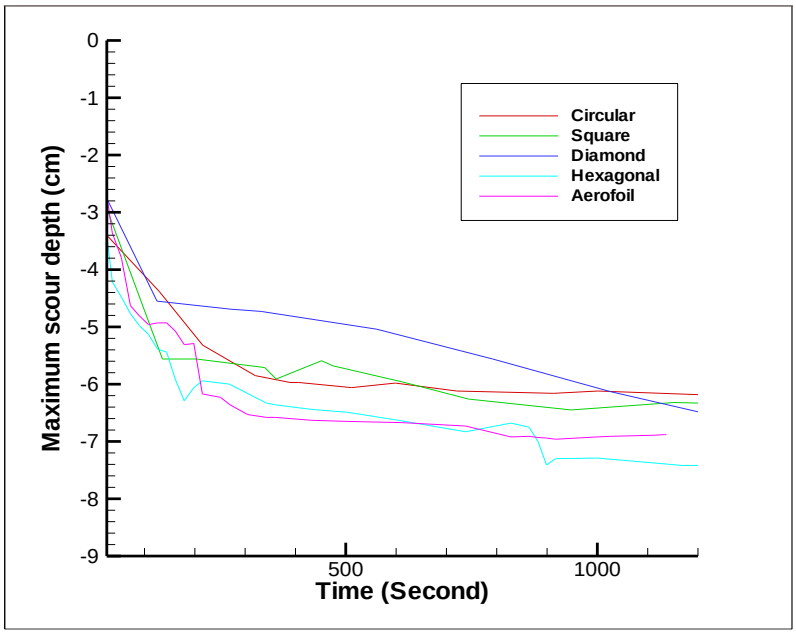

Figure 34:Comparison of numerical maximum scour depth(cm) among five piers structures

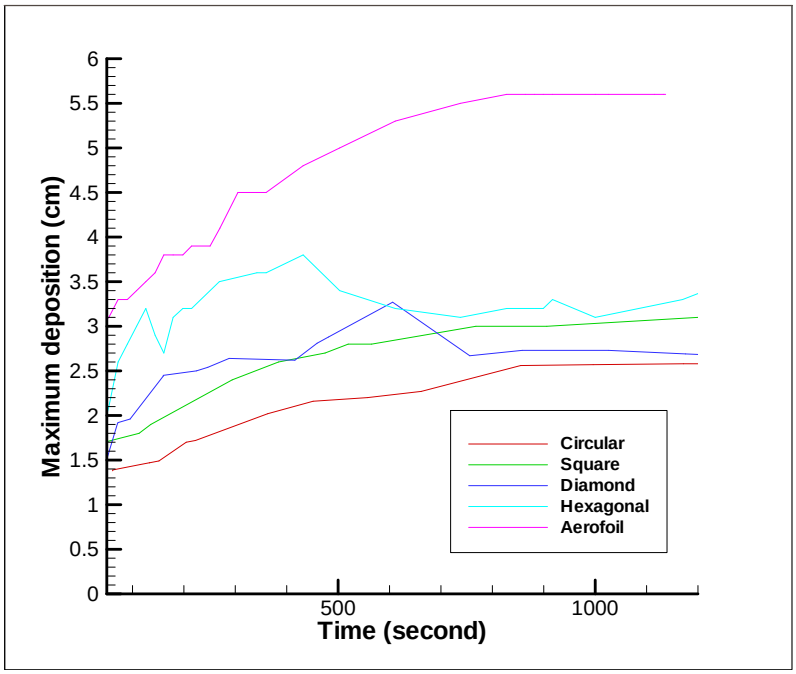

Figure 35:Comparison of numerical maximum deposition height(cm) among five piers structures

From the above comparison between five geometrical structures it is very clear that the lowest maximum scour depth has been observed in case of circular shape pier. And the result of maximum scour depth for the rest of the geometry is not satisfactory that can help us to reduce the scouring around bridge piers. So the current circular shape pier which has been used worldwide for so many years is the best one according to our study. Numerical values of that five structures are given below.

Shape of Bridge Piers	Maximum Scour Depth(Numerical)	Maximum Scour Depth (Experimental)[26]
Circular	6.5cm	6.7cm
Square	6.6cm	7.6cm
Diamond	8.5cm	8.3cm

Table 4: Numerical and experimental maximum scour depth(cm) for circular, square and diamond pier

Shape of Bridge Piers	Percentage of Error
Circular	2.98%
Square	13.15%
Diamond	2.40%

Table 5: Comparison between experimental and numerical result for maximum scour depth

Shape of Bridge Piers	Maximum Deposition Height (Numerical)	Maximum Deposition Height (Experimental)[26]
Circular	2.6cm	4.1cm
Square	2.9cm	5.5cm
Diamond	4.8cm	5.5cm

Table 6: Numerical and experimental maximum deposition height(cm) for circular, square and diamond pier

And the scour depth obtained from the two new case study model also has been mentioned down below.

Shape of Bridge Piers	Maximum Scour Depth	Maximum Deposition Height
Hexagonal	8.0cm	3.9cm
Airfoil	7.9cm	5.3cm

Table 7:Numerical maximum scour depth(cm) and maximum deposition height(cm) for hexagonal and airfoil pier

We can show another comparison among the rest four shapes by considering the circular pier as the best one.

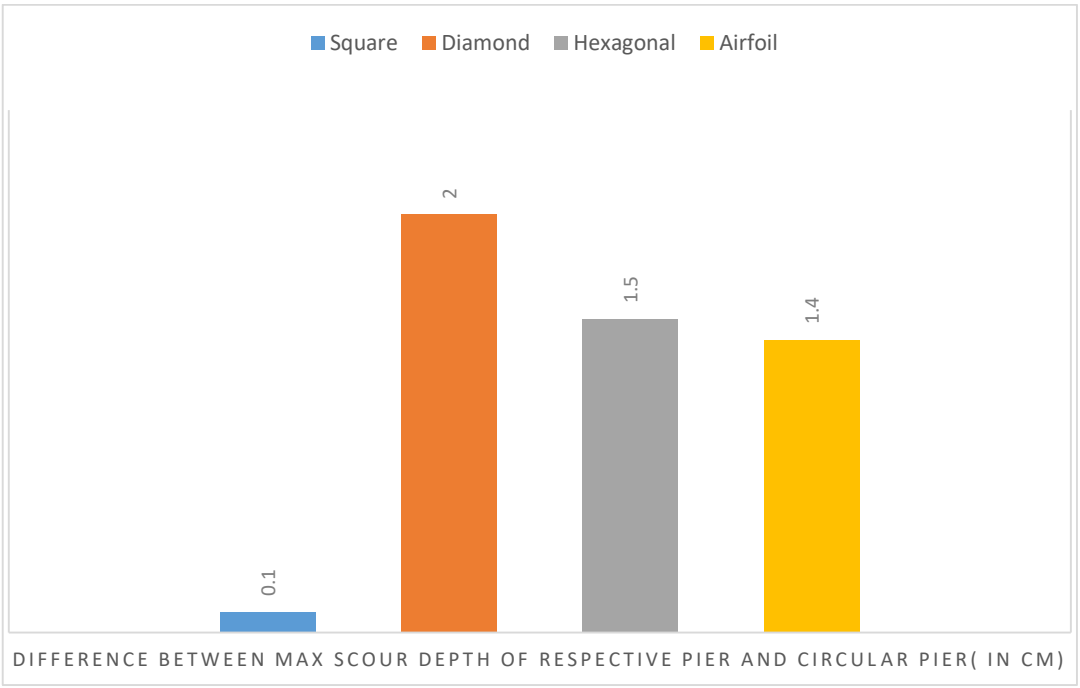

Figure 36: Comparison among square, diamond, hexagonal and airfoil piers

Chapter 6 Future Directions and Recommendations

Our main target of study is to lowering the scouring depth by decreasing the strength of impact of flow on the surface wall of the different pier structures. And with this hope we came up with another two structures and expecting that it will ensure the dropping of maximum scour depth. The two new models for study are circular shaped bridge piers with one collar around the pier and circular shaped bridge piers with two collars around the pier.

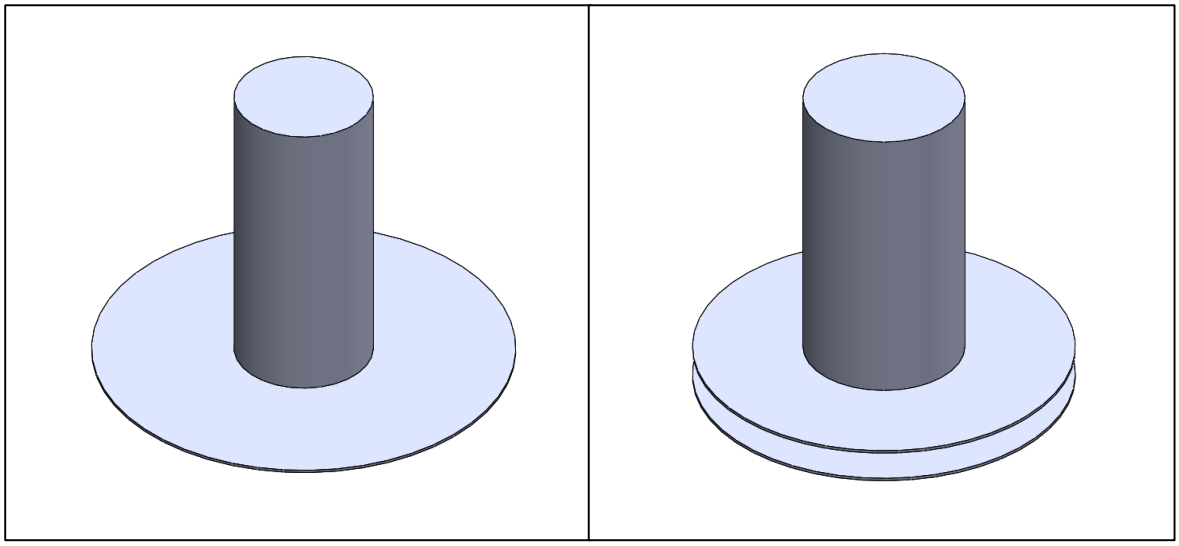

(a) (b)

Figure 37:(a)circular shaped bridge piers with one collar around pier and (b)circular shaped bridge piers with two collars around pier.

So more experimental and numerical studies should be done in future considering different diameter circular pier with different diameter collar at different position to find out in which case scouring effect become the lowest.

References

[1] J. Briaud, F. Ting, H. Chen, R. Gudavalli, S. Perugu and G. Wei, "SRICOS: Prediction of Scour Rate in Cohesive Soils at Bridge Piers", *Journal of Geotechnical and Geoenvironmental Engineering*, vol. 125, no. 4, pp. 237-246, 1999. Available: 10.1061/(asce)1090-0241(1999)125:4(237)

[2] Baker C. The turbulent horseshoe vortex. J Wind Eng Indus Aerodyn 1980;6:9–23.

[3] Devenport WJ, Simpson RL. Time-dependent and time-averaged turbulence structure near the nose of a wing-body junction. J Fluid Mech 1990;210(2):23–55.

[4] J. Agui and J. Andreopoulos, "Experimental Investigation of a Three-Dimensional Boundary Layer Flow in the Vicinity of an Upright Wall Mounted Cylinder (Data Bank Contribution)", *Journal of Fluids Engineering*, vol. 114, no. 4, pp. 566-576, 1992. Available: 10.1115/1.2910069.

[5] Doligalski TL, Smith CR, Walker JDA. Vortex interactions with walls. Ann Rev Fluid Mech 1994;26:573–616.

[6] Seal CV, Smith CR. Visualization of a mechanism for three-dimensional interaction and near-wall eruption. J Fluid Mech 1999;394:193–203.

[7] Martinuzzi R, Tropea C. The flow around surface-mounted, prismatic obstacles placed in a fully developed channel flow. J Fluids Eng 1993;115:85–92.

[8] Hussein H, Martinuzzi R. Energy balance for turbulent flow around a surface mounted cube placed in a channel. Phys Fluids 1996;8:764–80.

[9] Unger J, Hager WH. Down-flow and horseshoe vortex characteristics of sediment embedded bridge piers. Exp Fluids 2007;42(1):119.

[10] Mendoza-Cabrales C. Computation of flow past a cylinder mounted on a flat plate. In: ASCE Hydraulic engineering, proceedings of national conference.

[11]Richardson JE, Panchang VG. Three-dimensional simulation of scour-inducing flow at bridge piers. J Hydraul Eng 1998;124(5):530–40.

[12]Tseng MH, Yen CL, Song CCS. Computation of three-dimensional flow around square and circular piers. Int J Numer Methods Fluids 2000;34:207–27.

[13]Nurtjahyo PY. Numerical Simulation of Pier Scour and Contraction Scour, Ph.D. thesis, Department of Civil Engineering, Texas A&M University, Texas; 2002.

[14] Ge L, Sotiropoulos F. 3d unsteady RANS modeling of complex hydraulic engineering flows. part i: Numerical model. J Hydraul Eng 2005;131(9):800–8.

[15]Salaheldin TM, Imran J, Chaudhry MH. Numerical modeling of three-dimensional flow field around circular piers. J Hydraul Eng 2004; 130(2):91100.

[16]https://www.usgs.gov/media/images/scour-hole-around-bridge-pier

[17]https://www.jbatrust.org/wp-content/uploads/2016/01/JBA-Trust-Flood-and scour-failure-at-railway-assets-1846-to-2013-W13-4224-FINAL.pdf

[18] Shirhole, A. M., and Holt, R. C. “Planning for a comprehensive bridge safety program.” Transportation Research Record No. 1290, Transportation Research Board, National Research Council, Washington, D.C. 1991

[19] Lagasse, P. F., Richardson, E. V., Schall, J. D., and Price, G. R. “Instrumentation for measuring scour at bridge piers and abutments.” National Cooperative Highway Research Program (NCHRP) Report No. 396, Transportation Research Board, Washington, D.C 1997

[20] Alabi, P.D. Time development of local scour at bridge pier fitted with a collar. Master Science Thesis, University of Saskatchewan, Canada 2006

[21] Briaud, J.L., Gardoni, P., Yao, C. . Bridge Scour Risk, ICSE6 Paris. ICSE6-011 -2012

[22] K. Subramanya, *Flow in open channels*, 3rd ed. New Delhi: McGraw Hill Education (India), 2015, pp. 483-485.

[23] https://en.wikipedia.org/wiki/Bridge_scour

[24] B. Melville and S. Coleman, *Bridge scour*. 2000.

[25] G. Wei, J. Brethour, M. Grünzner and J. Burnham, "Sedimentation Scour Model", *Flow Science Report 03-14*, 2014.

[26] A. Khosronejad, S. Kang and F. Sotiropoulos, "Experimental and computational investigation of local scour around bridge piers", *Advances in Water Resources*, vol. 37, pp. 73-85, 2012. Available: 10.1016/j.advwatres.2011.09.013.

[27] Melville BW, Chiew YM. Time scale for local scour at bridge piers. J Hydraul Eng 1999;125(1):59–65.

[28] Dargahi B. Controlling mechanism of local scouring. J Hydraul Eng 1990;116(10):1197–214.

[29] Roulund A, Sumer BM, Fredsoe J, Michelsen J. Numerical and experimental investigation of flow and scour around a circular pile. J Fluid Mech 2005;534:351–401.

[30] Ram, S. "A Theoretical Model to Predict Local Scour at Bridge Piers in Non-cohesive Soils." *Proc., River Sedimentation Theory and Application,* A.A. Balkema, Rotterdam, Brook Field, 173-178,1999

[31] Melville, B.W. and Chiew, YM. . "Time Scale of Local Scour around Bridge Piers." *J. of Hydraulic Engineering.* ASCE, 125(1),59-65,1999

[32] Kothyari, U.C., Garde, R.C.J., and Raju, K.G.R. (1992a). "Temporal Variation of Scour around Circular Bridge Piers." *J. of Hydraulic Engineering,* ASCE, I 18(8), 1091-1105.

[33] Johnson, P.A. and Bilal, M.A. "Assessing Time Variant Bridge Reliability due to Pier Scour." *J. of Hydraulic Engineering,* ASCE, 118(6), 887-903,1992

[34] Laursen, E.M."An Analysis of Relief Bridge Scour." *J. of Hydraulic Engineering,* ASCE, 89(3), 93-118,1963

[35] Vittal, N., Kothyari, *V.c.* and Haghighat, M. "Clear Water Scour around Bridge Pier Group." 1. *of Hydraulic Engineering,* ASCE, 120(11), 1309-1318,1994

[36] Jain, S.c. and Fischer, E.E. "Scour around Bridge Piers at High Flow Velocities." *J. of Hydraulic Engineering,* ASCE, 106(11), 1827-1842,1981

[37] Kothyari, U.c., Garde, R.C.J. and Raju, K.G.R. (1992b). "Live Bed Scour around Cylindrical Bridge Piers." *Journal of Hydraulic Research,* IAHR, 30 (5),701 715.

[38] Laursen, E.M. "Scour at Bridge Crossings." *Trans.,* 127(I), ASCE, Paper 3294,1962

[39] Molinas, A. and Abdeldayem, A. "Effect of Clay Content on Bridge Scour." *J. of Water Resources Engineering,* ASCE, 1,280-285,1998

[40] Raudkivi, A.J. and Ettema, R. "Effects of Sediment Gradation on Clear Water Scour." 1. *of Hydraulic Engineering,* ASCE, 103(10), 1209-1212,1977

[41] Kabir, M.R., Faisal, I.M. and Khatun, F. "Laboratory Study and Field Investigation of Scour around Bridge pier in Bangladesh." Proc., *International Symposium on Scour of Foundations,* IS-Scour 2000, ISSMGE, TC-33, Melbourne, Australia.

[42] Kandasamy, J.K. and Melville, B.W. "Maximum Local Scour Depth at Bridge Piers and Abutments." *Journal of Hydraulic Research,* IAHR, 36(2), 183-198,1998

[43] Melville, B.W. and Sutherland, A.J. "Design Method for Local Scour at Bridge Piers." *J. of Hydraulic Engineering,* ASCE, 114(10), 1210-1227,1988

[44] Chang, H.H.. "Fluvial Processes in River Engineering." John Wiley & Sons, Inc, USA, 96-99,1988

[45] Garde, R.J. and Raju, K.G.R. "Mechanics of Sediment Transportation and Alluvial Stream Problem", 2nd Edition, Wiley Eastern Ltd., New Delhi, India,1985

[46] Johnson, P.A. and Bilal, M.A. "Assessing Time Variant Bridge Reliability due to Pier Scour." *J. of Hydraulic Engineering,* ASCE, 118(6), 887-903,1992

[47] Dey, S., Bose, S.K. and Sastry, G.L.N. "Clear Water Scour at Circular Piers: A Model." *J. of Hydraulic Engineering,* ASCE, 121(12), 869-876,1995

[48] Sheppard, D.M. and Jones, J.S. "Scour at Complex Pier Geometries." *J. of Water Resources Engineering,* ASCE, 1, 192-197,1998

[49] Kumar, V., Raju, K.G.R. and Vittal, N. "Reduction of Local Scour around Bridge Piers using Slots and Collars." *J. of Hydraulic Engineering,* ASCE, 125(12), 1302-1305,1999

[50] Parola, A.C., Mahavadi, S.K., Brown, B. M. and Khoury, A.E. "Effects of Rectangular Foundation Geometry on Local Pier Scour." *J. Of Hydraulic Engineering,* ASCE, 122(1), 35-40,1996

[51] Lim, S.Y. and Chiew, YM. (1999). "Effects of an Upstream Pile on Pier Scour." *Proc River Sedimentation The OlY and Application,* A.A. Balkema, Rotterdam, Brook Field, 153-158.

[52] Flow-3D documentation